Lattice QCD Calculation of Electroweak Box Contributions

Based on Phys. Rev. Lett. 132, 191901.

Speaker: Peng-Xiang Ma

Co-Author: Xu Feng, Mikhail Gorchtein, Lu-Chang Jin, Keh-Fei Liu,
Chien-Yeah Seng, Bi-Geng Wang and Zhaolong Zhang

Institute of Theoretical Physics， Peking University

CKM Unitarity

北京大学 PEKING UNIVERSITY

- CKM matrix plays a crucial role as fundamental parameters of the standard model:

$$\begin{bmatrix} d' \\ s' \\ b' \end{bmatrix} = \begin{bmatrix} V_{ud} & V_{us} & V_{ub} \\ V_{cd} & V_{cs} & V_{cb} \\ V_{td} & V_{ts} & V_{tb} \end{bmatrix} \begin{bmatrix} d \\ s \\ b \end{bmatrix}$$

- The unitarity test of the CKM matrix serves as one of the most important precision tests in particle physics.

- The first row of the CKM matrix provides the most accurate result:

$$|V_{ud}|^2 + |V_{us}|^2 + |V_{ub}|^2 = 0.9985(6)_{V_{ud}}(4)_{V_{us}}, \quad (|V_{ub}|^2 \simeq 1.7 \times 10^{-5} \ll 1).$$

- V_{ud} could be derived from nuclear and neutron beta decay.

- V_{us} could be derived from $K_{\mu 2}$ and K_{l3} decays.

from Lattice $\quad \dfrac{f_{K^+}}{f_{\pi^+}} \dfrac{|V_{us}|}{|V_{ud}|} = 0.27600(37), \quad$ from $K_{\mu 2}$.

from Lattice $\quad f_+(0)|V_{us}| = 0.21635(38)(3), \quad$ from $K_{\ell 3}$.

Experimental Input for V_{ud}

$|V_{ud}|$

Experimental Input for V_{ud}

$$|V_{ud}|$$

$$0^+ \rightarrow 0^+$$

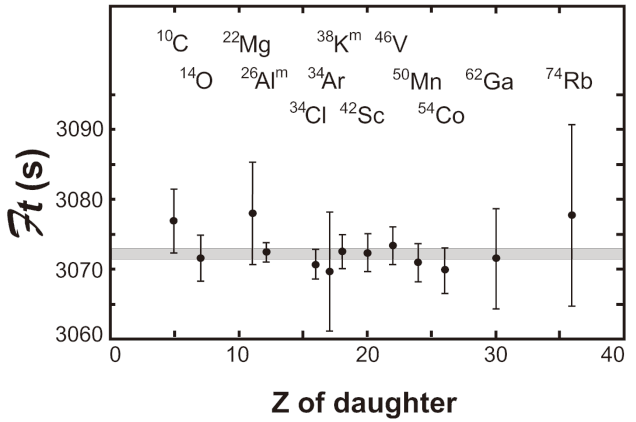

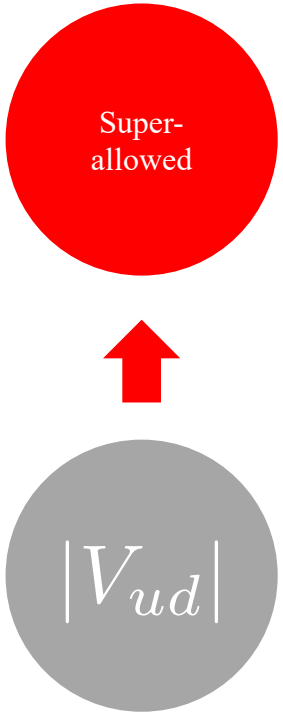

Experimental Input for V_{ud}

$$0^+ \rightarrow 0^+$$

- Three ways to extract $|V_{ud}|$:
  - Super-allowed beta decay:
    - most accurate
    - limited by nuclear structure(NS)

$$|V_{ud}|^2 = \frac{0.97154(22)_{\mathrm{exp}}(54)_{\mathrm{NS}}}{(1+\Delta_R^V)}, \quad \text{superallowed,}$$

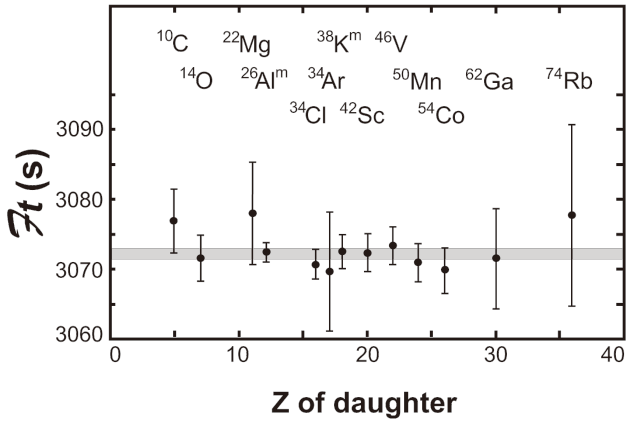

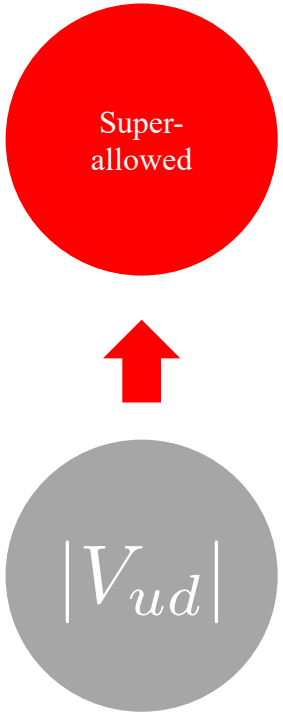

  - Ultra-Cold Neutron:
    - universal RC with super-allowed
    - not limited by NS, but limited by g_A

  - PIBETA & PIONEER:
    - Theoretically clean
    - limited by experimental input

Experimental Input for V_{ud}

$$0^+ \rightarrow 0^+$$

- Three ways to extract $|V_{ud}|$:
  - Super-allowed beta decay:
    - most accurate
    - limited by nuclear structure(NS)

$$|V_{ud}|^2 = \frac{0.97154(22)_{\mathrm{exp}}(54)_{\mathrm{NS}}}{(1+\Delta_R^V)}, \quad \text{superallowed},$$

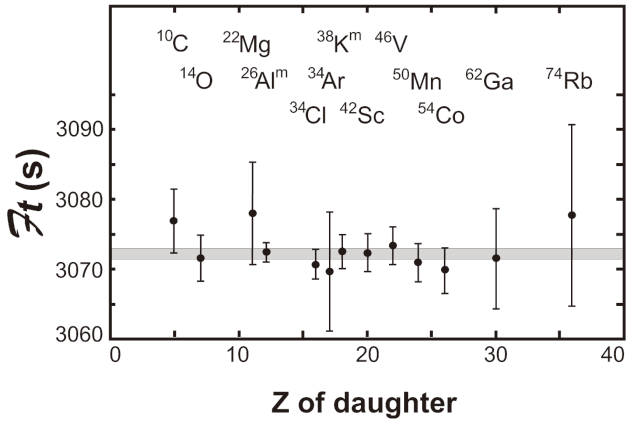

  - Ultra-Cold Neutron:
    - universal RC with super-allowed
    - not limited by NS, but limited by g_A

  - PIBETA & PIONEER:
    - Theoretically clean
    - limited by experimental input

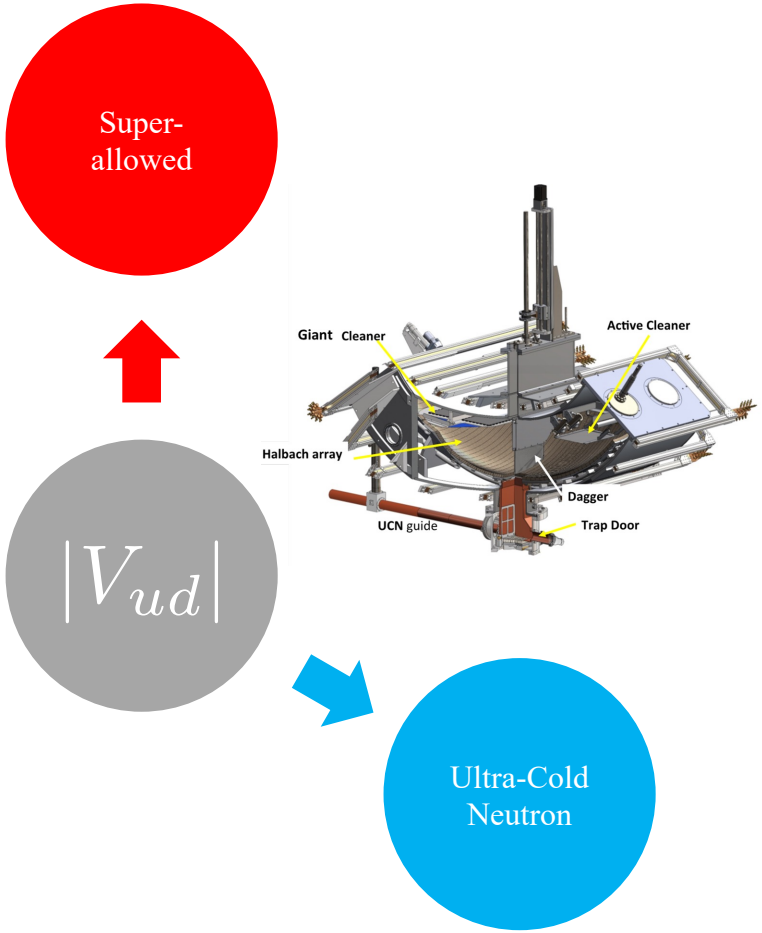

Experimental Input for V_{ud}

$$0^+ \rightarrow 0^+$$

- Three ways to extract $|V_{ud}|$:
  - Super-allowed beta decay:
    - most accurate
    - limited by nuclear structure(NS)

$$|V_{ud}|^2 = \frac{0.97154(22)_{\exp}(54)_{\mathrm{NS}}}{(1+\Delta_R^V)}, \quad \text{superallowed},$$

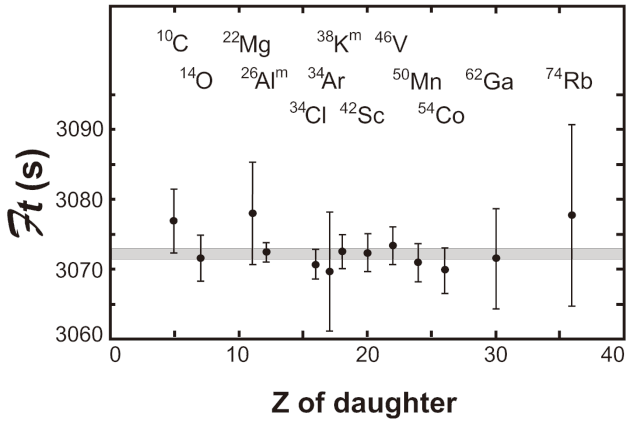

  - Ultra-Cold Neutron:
    - universal RC with super-allowed
    - not limited by NS, but limited by g_A

$$|V_{ud}|^2 = \frac{0.9728(6)_{\tau_n}(16)_{g_A}}{(1+\Delta_R^V)}, \quad \text{free neutron.}$$

  - PIBETA & PIONEER:
    - Theoretically clean
    - limited by experimental input

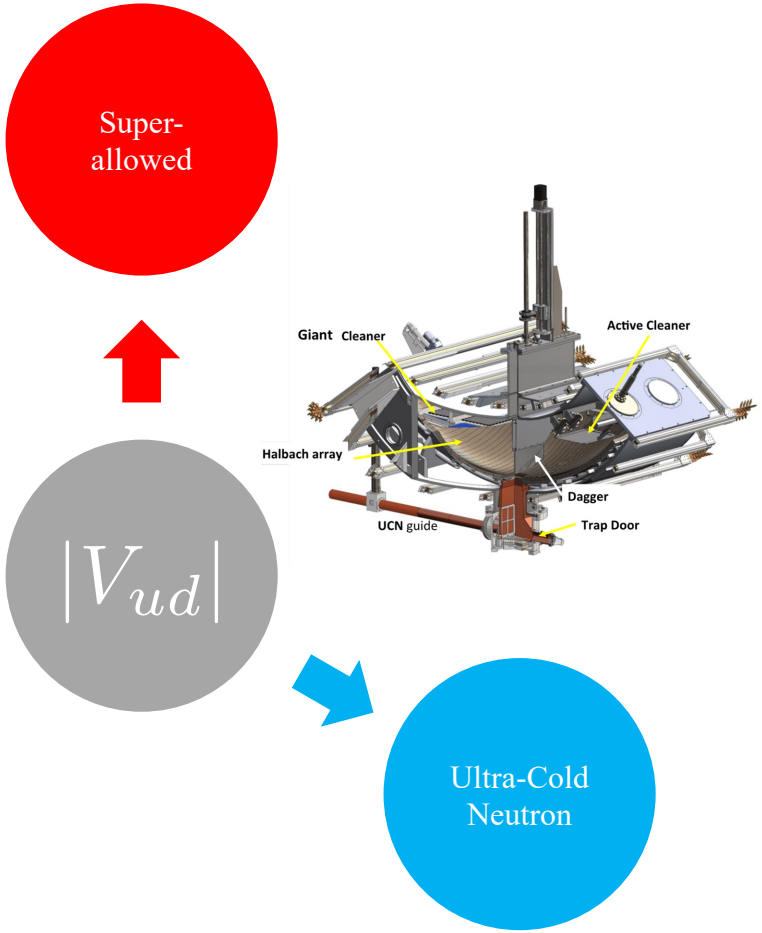

Experimental Input for V_{ud}

$$0^+ \rightarrow 0^+$$

- Three ways to extract $|V_{ud}|$:
  - Super-allowed beta decay:
    - most accurate
    - limited by nuclear structure(NS)

$$|V_{ud}|^2 = \frac{0.97154(22)_{\rm exp}(54)_{\rm NS}}{(1+\Delta_R^V)}, \quad \text{superallowed},$$

  - Ultra-Cold Neutron:
    - universal RC with super-allowed
    - not limited by NS, but limited by g_A

$$|V_{ud}|^2 = \frac{0.9728(6)_{\tau_n}(16)_{g_A}}{(1+\Delta_R^V)}, \quad \text{free neutron}.$$

  - PIBETA & PIONEER:
    - Theoretically clean
    - limited by experimental input

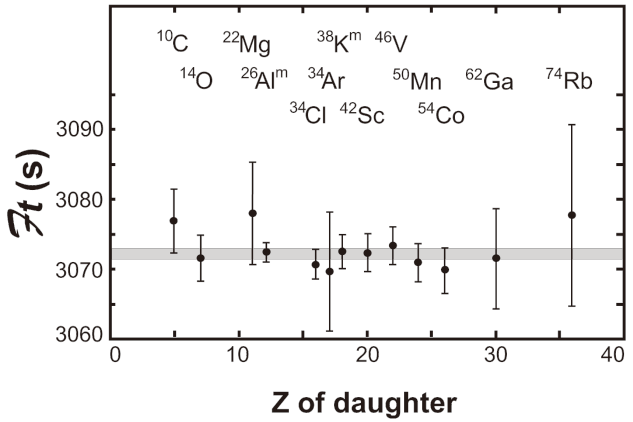

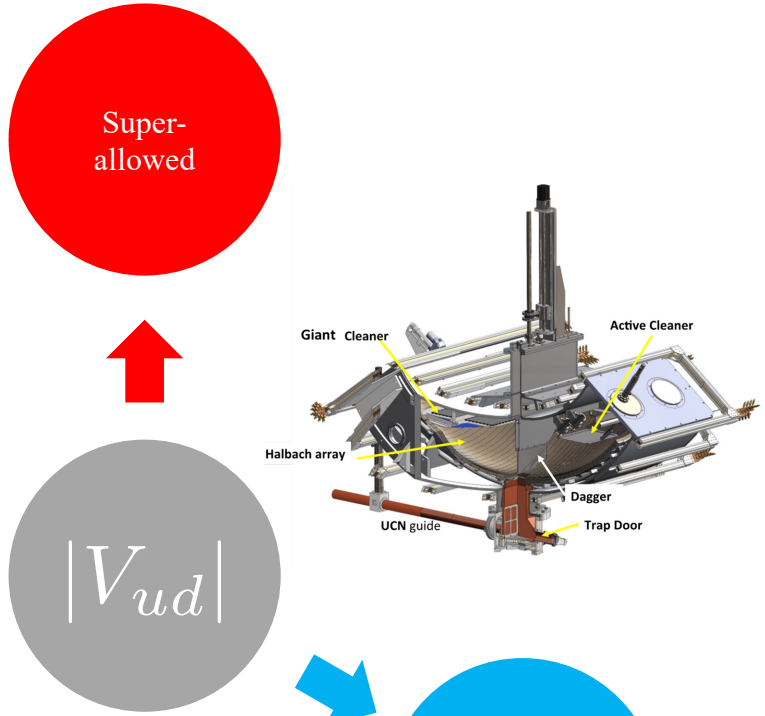

Experimental Input for V_{ud}

$$0^+ \rightarrow 0^+$$

- Three ways to extract $|V_{ud}|$:
  - Super-allowed beta decay:
    - most accurate
    - limited by nuclear structure(NS)

$$|V_{ud}|^2 = \frac{0.97154(22)_{\rm exp}(54)_{\rm NS}}{(1+\Delta_R^V)}, \quad \text{superallowed},$$

  - Ultra-Cold Neutron:
    - universal RC with super-allowed
    - not limited by NS, but limited by g_A

$$|V_{ud}|^2 = \frac{0.9728(6)_{\tau_n}(16)_{g_A}}{(1+\Delta_R^V)}, \quad \text{free neutron}.$$

  - PIBETA & PIONEER:
    - Theoretically clean
    - limited by experimental input

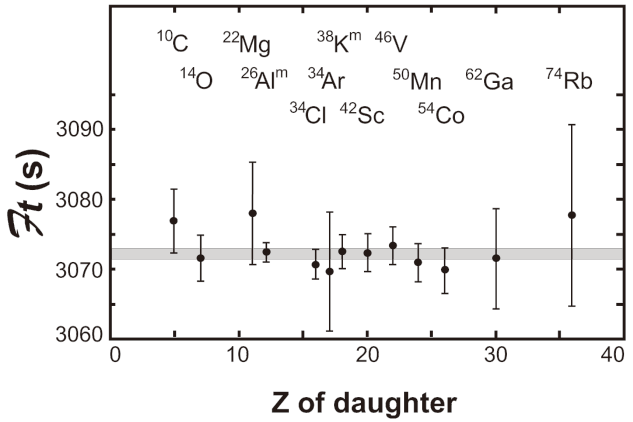

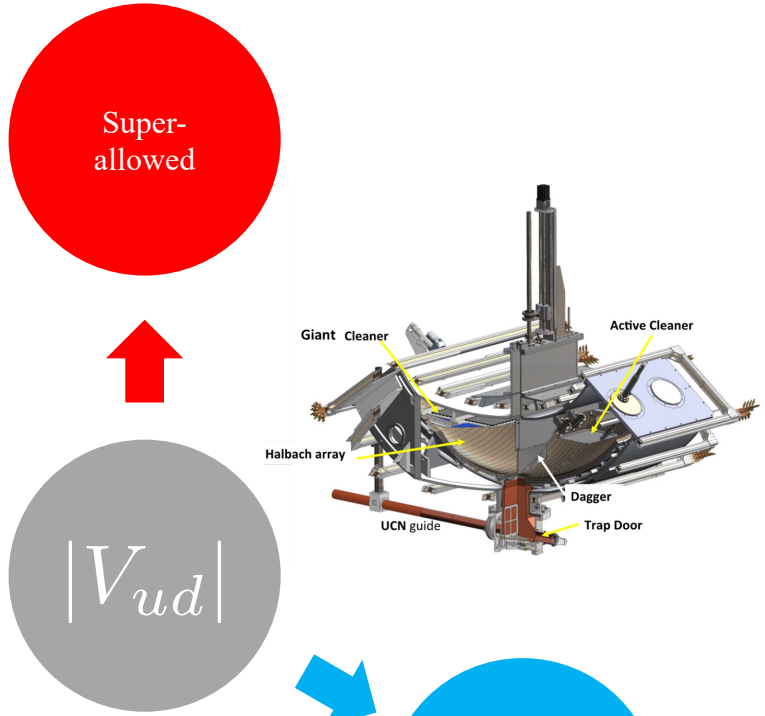

PDG 2019 ~ 2022

北京大学 PEKING UNIVERSITY

PDG	$\lvert V_{ud}\rvert$	$\lvert V_{us}\rvert$	CKM Unitarity	Discrepancy
2019				
2020				
2022				

PDG 2019 ~ 2022

北京大学 PEKING UNIVERSITY

PDG	$\lvert V_{ud}\rvert$	$\lvert V_{us}\rvert$	CKM Unitarity	Discrepancy
2019	$0.97420(10)_{\mathrm{exp}}(18)_{\mathrm{RC}}$	$0.2243(5)$	$0.9994(4)(2)$	$1.4\ \sigma$
2020				
2022				

PDG 2019 ~ 2022

北京大学 PEKING UNIVERSITY

PDG	$\lvert V_{ud}\rvert$	$\lvert V_{us}\rvert$	CKM Unitarity	Discrepancy
2019	$0.97420(10)_{\mathrm{exp}}(18)_{\mathrm{RC}}$	$0.2243(5)$	$0.9994(4)(2)$	$1.4\ \sigma$
2020	$0.97370(10)_{\mathrm{exp}}(10)_{\mathrm{RC}}$	$0.2245(8)$	$0.9985(3)(4)$	$3.3\ \sigma$
2022				

PDG 2019 ~ 2022

北京大学 PEKING UNIVERSITY

PDG	$\lvert V_{ud}\rvert$	$\lvert V_{us}\rvert$	CKM Unitarity	Discrepancy
2019	$0.97420(10)_{\rm exp}(18)_{\rm RC}$	$0.2243(5)$	$0.9994(4)(2)$	$1.4\ \sigma$
2020	$0.97370(10)_{\rm exp}(10)_{\rm RC}$	$0.2245(8)$	$0.9985(3)(4)$	$3.3\ \sigma$
2022				

PDG 2019 ~ 2022

PDG	$\lvert V_{ud}\rvert$	$\lvert V_{us}\rvert$	CKM Unitarity	Discrepancy
2019	$0.97420(10)_{\rm exp}(18)_{\rm RC}$	$0.2243(5)$	$0.9994(4)(2)$	$1.4\ \sigma$
2020	$0.97370(10)_{\rm exp}(10)_{\rm RC}$	$0.2245(8)$	$0.9985(3)(4)$	$3.3\ \sigma$
2022	$0.97373(10)_{\rm exp}(10)_{\rm RC}(27)_{\rm NS}$	$0.2243(8)$	$0.9985(6)(4)$	$2.2\ \sigma$

PDG 2019 ~ 2022

北京大学 PEKING UNIVERSITY

➢ PDG made several updates for CKM unitarity these years:

PDG	$\lvert V_{ud}\rvert$	$\lvert V_{us}\rvert$	CKM Unitarity	Discrepancy
2019	$0.97420(10)_{\rm exp}(18)_{\rm RC}$	$0.2243(5)$	$0.9994(4)(2)$	$1.4\ \sigma$
2020	$0.97370(10)_{\rm exp}(10)_{\rm RC}$	$0.2245(8)$	$0.9985(3)(4)$	$3.3\ \sigma$
2022	$0.97373(10)_{\rm exp}(10)_{\rm RC}(27)_{\rm NS}$	$0.2243(8)$	$0.9985(6)(4)$	$2.2\ \sigma$

➢ V_{us} in this table is from the average of $K_{\mu 2}$ and K_{l3} decays.

$$\begin{cases} |V_{us}| = 0.2252(5) & K_{\mu 2} \\ |V_{us}| = 0.2243(4) & K_{\ell 3} \end{cases}$$

differ by ~ 2 σ

a scale factor of 2.7 →

$$|V_{us}| = 0.2243(8)$$

EWRC from Dispersion Relation Analysis

$$\Box_{\gamma W}^{VA}\big|_H = \frac{3\alpha_e}{2\pi}\int \frac{dQ^2}{Q^2}\frac{m_W^2}{m_W^2+Q^2}M_H\left(Q^2\right)$$

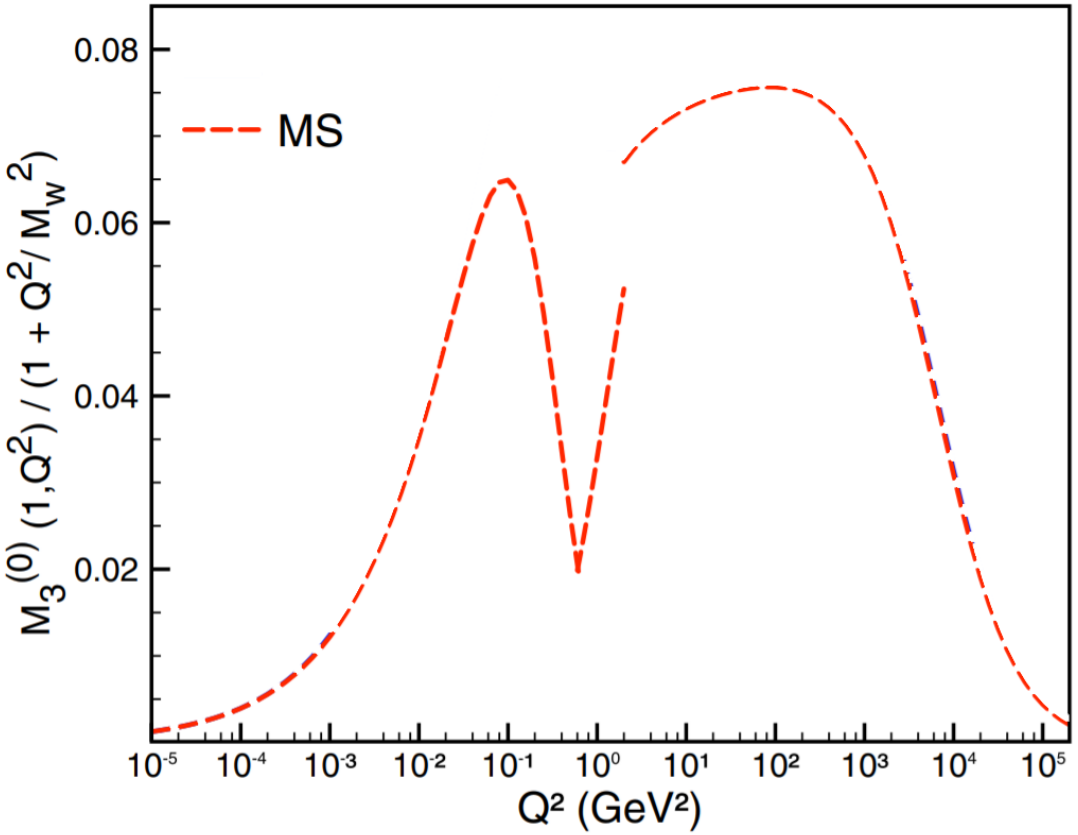

Marciano and Sirlin[1],
vector dominance model(VDM).

$$\left|V_{ud}^{\text{old}}\right| = 0.97420(18)_{\text{RC}}\,(10)_{\mathcal{F}t}$$

Phys. Rev. Lett. 96, 032002 (2006).

EWRC from Dispersion Relation Analysis

$$\Box_{\gamma W}^{VA}\big|_H = \frac{3\alpha_e}{2\pi}\int \frac{dQ^2}{Q^2}\frac{m_W^2}{m_W^2+Q^2}M_H\left(Q^2\right)$$

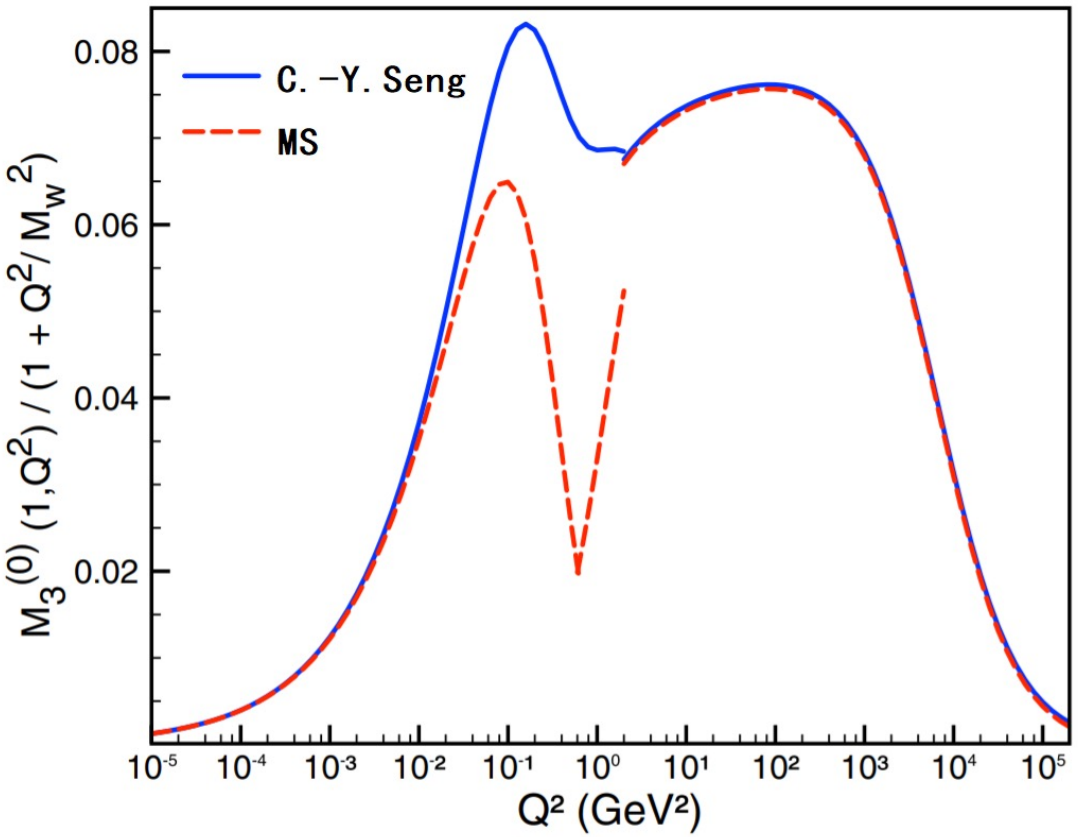

Marciano and Sirlin[1],
vector dominance model(VDM).

$$|V_{ud}^{\text{old}}| = 0.97420(18)_{\text{RC}}\,(10)_{\mathcal{F}t}$$

Phys. Rev. Lett. 96, 032002 (2006).

C.-Y. Seng, M. Gorchtein and M. J. Ramsey-Musolf[2].
dispersion relation & data-driven analysis.

$$|V_{ud}^{\text{new}}| = 0.97370(10)_{\text{RC}}\,(10)_{\mathcal{F}_t}$$

Phys. Rev. Lett. 121, no.24, 241804 (2018).

EWRC from Dispersion Relation Analysis

$$\Box_{\gamma W}^{VA}\big|_H = \frac{3\alpha_e}{2\pi}\int \frac{dQ^2}{Q^2}\frac{m_W^2}{m_W^2+Q^2}M_H\left(Q^2\right)$$

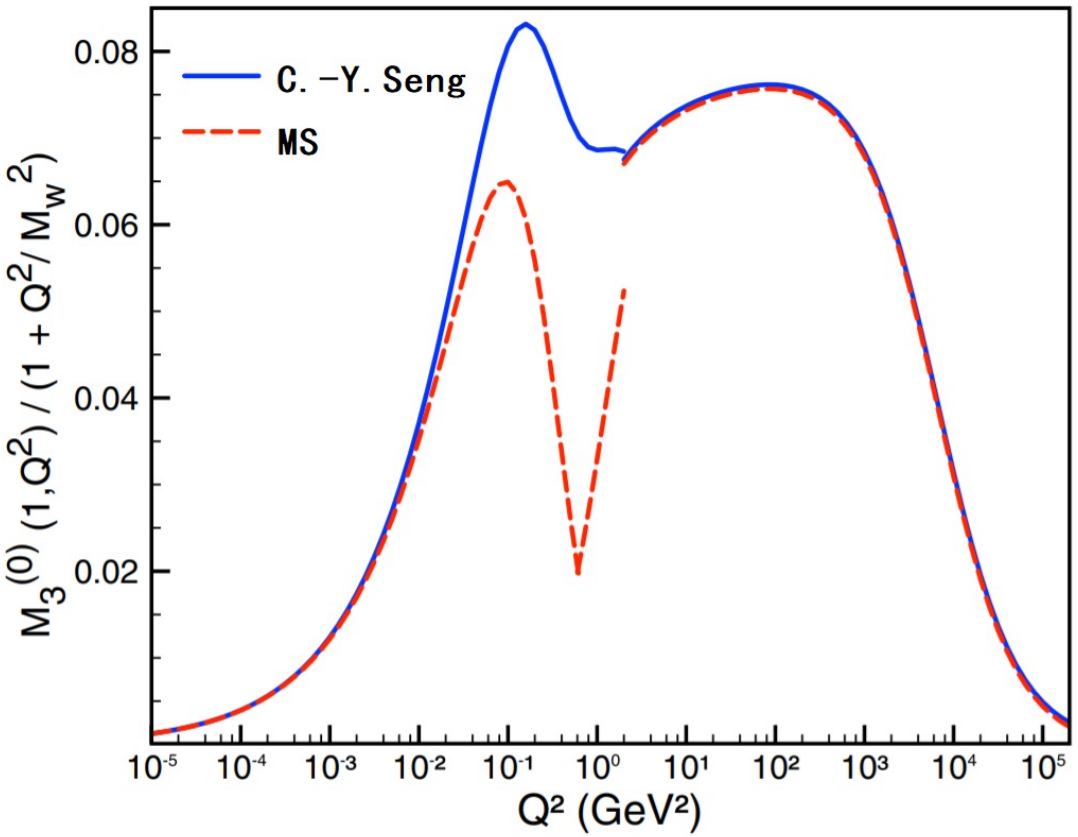

Marciano and Sirlin[1],
vector dominance model(VDM).

$$|V_{ud}^{\text{old}}| = 0.97420(18)_{\text{RC}}\,(10)_{\mathcal{F}t}$$

Phys. Rev. Lett. 96, 032002 (2006).

C.-Y. Seng, M. Gorchtein and M. J. Ramsey-Musolf[2].
dispersion relation & data-driven analysis.

$$|V_{ud}^{\text{new}}| = 0.97370(10)_{\text{RC}}\,(10)_{\mathcal{F}_t}$$

Phys. Rev. Lett. 121, no.24, 241804 (2018).

first principle calculation

γW-box Diagram

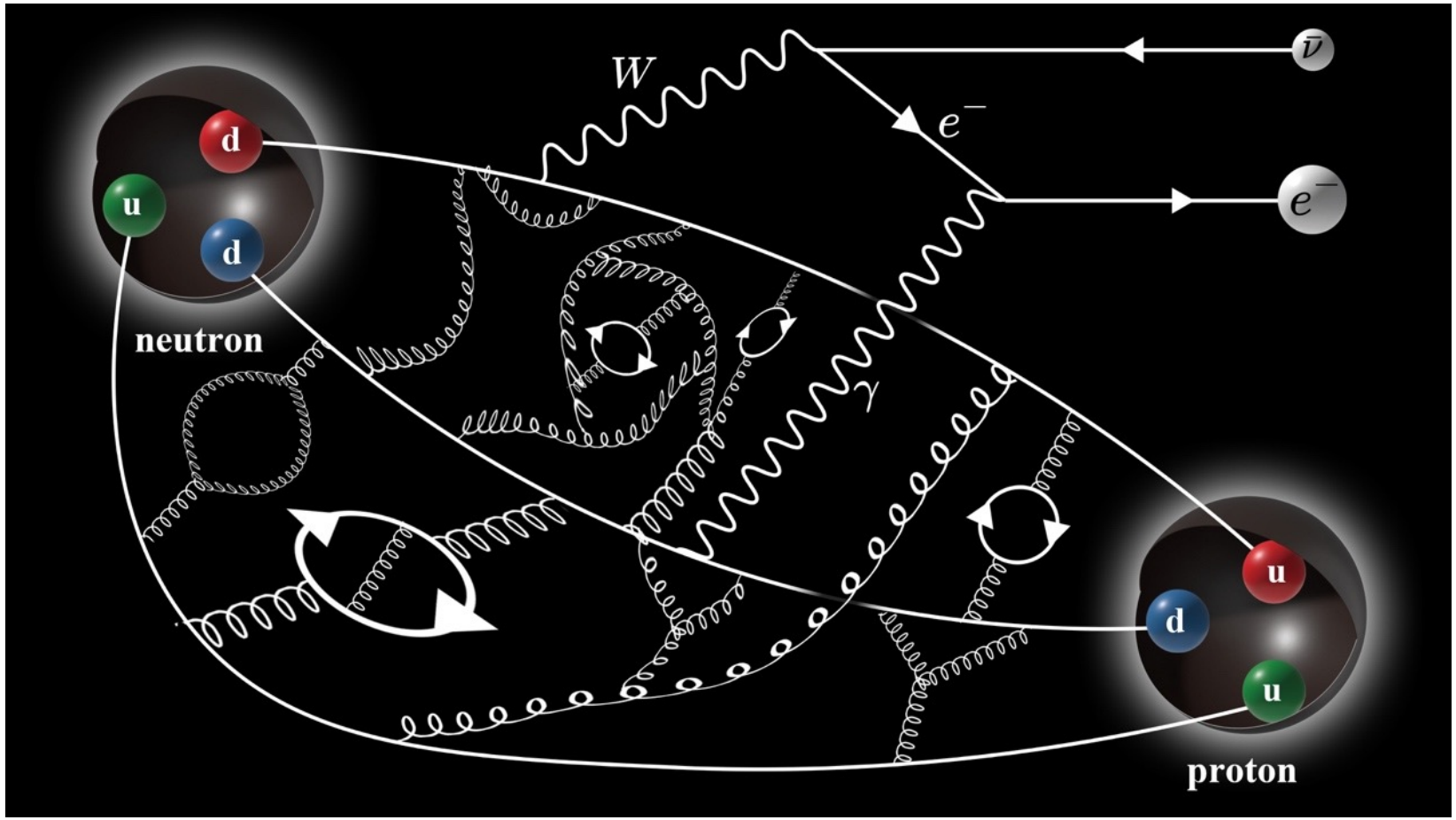

➢ γW-box diagram for neutron beta decays. Non-perturbative hadronic effects happen here.

Axial γW-box Correction

- The nucleus-independent electroweak term dominates the uncertainty of radiative correction, which is universal for both nuclear and free neutron beta decay.

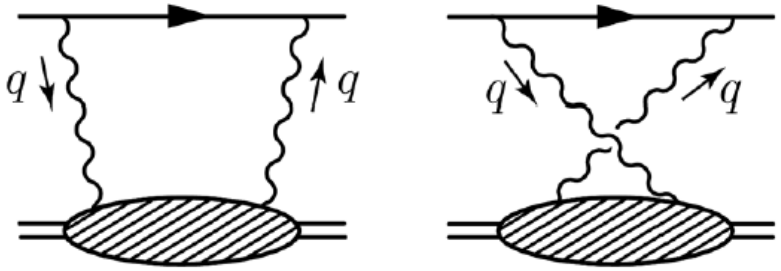

- According to Sirlin*, among various contributions, only the axial γW-box contribution is sensitive to hadronic scales

A. Sirlin, Rev. Mod. Phys. 50, 573 (1978).

Axial γW-box Correction

- The nucleus-independent electroweak term dominates the uncertainty of radiative correction, which is universal for both nuclear and free neutron beta decay.

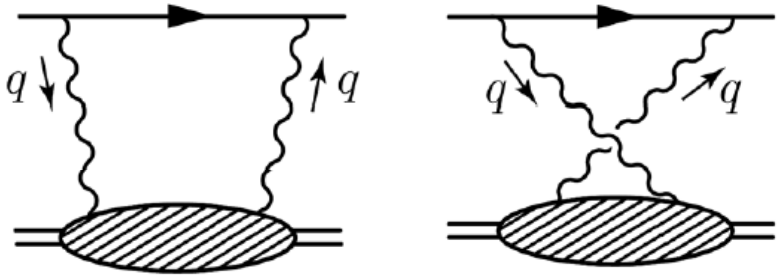

- According to Sirlin*, among various contributions, only the axial γW-box contribution is sensitive to hadronic scales

A. Sirlin, Rev. Mod. Phys. 50, 573 (1978).

Axial γW-box Correction

- The nucleus-independent electroweak term dominates the uncertainty of radiative correction, which is universal for both nuclear and free neutron beta decay.

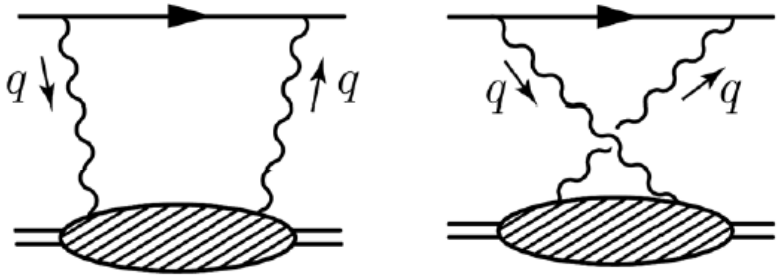

- According to Sirlin*, among various contributions, only the axial γW-box contribution is sensitive to hadronic scales

A. Sirlin, Rev. Mod. Phys. 50, 573 (1978).

$$T_{\mu\nu}^{VA} = \frac{1}{2}\int d^4x e^{iqx} \left\langle H_f(p) \left| T\left[J_\mu^{em}(x) J_\nu^{W,A}(0)\right] \right| H_i(p) \right\rangle$$

$$J_\mu^{em} = \frac{2}{3}\bar{u}\gamma_\mu u - \frac{1}{3}\bar{d}\gamma_\mu d \quad J_\nu^{W,A} = \bar{u}\gamma_\nu\gamma_5 d$$

Axial γW-box Correction

北京大学 PEKING UNIVERSITY

- The nucleus-independent electroweak term dominates the uncertainty of radiative correction, which is universal for both nuclear and free neutron beta decay.

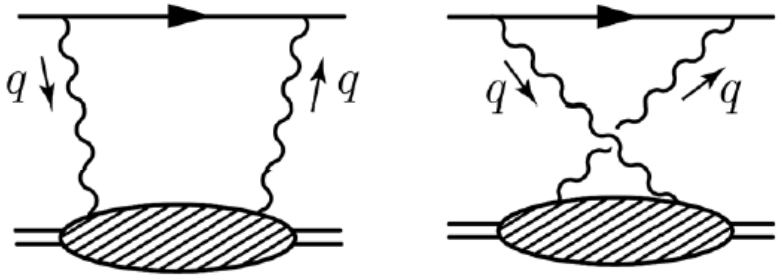

- According to Sirlin*, among various contributions, only the axial γW-box contribution is sensitive to hadronic scales

A. Sirlin, Rev. Mod. Phys. 50, 573 (1978).

$$T_{\mu\nu}^{VA} = \frac{1}{2}\int d^4x e^{iqx} \left\langle H_f(p) \left| T\left[J_\mu^{em}(x) J_\nu^{W,A}(0)\right] \right| H_i(p) \right\rangle \Rightarrow M_H(Q^2)$$

$$J_\mu^{em} = \frac{2}{3}\bar{u}\gamma_\mu u - \frac{1}{3}\bar{d}\gamma_\mu d \quad J_\nu^{W,A} = \bar{u}\gamma_\nu\gamma_5 d$$

Review of the Result of Pion Channel

- Box term could be expressed as a momentum integral for $M_H(Q^2)$:

$$\Box_{\gamma W}^{VA}\big|_H = \frac{3\alpha_e}{2\pi}\int \frac{dQ^2}{Q^2}\frac{m_W^2}{m_W^2+Q^2}M_H\left(Q^2\right)$$

- The uncertainty for the non-perturbative part was estimated by low energy constants from chiral perturbation theory.

- We calculated the box term for pion channel*, which reduced the uncertainty for the non-perturbative part by a factor of 10.

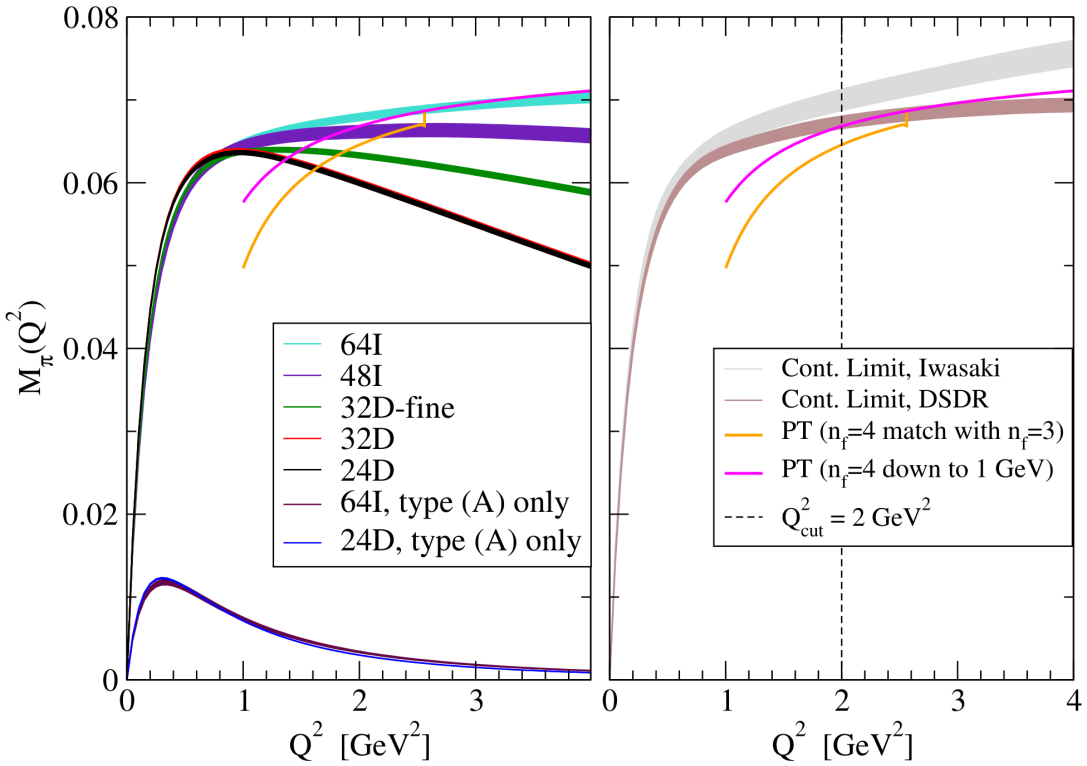

X. Feng, M. Gorchtein, L. C. Jin, P. X. Ma and C. Y. Seng, Phys. Rev. Lett. 124, no.19, 192002 (2020).

- This calculation has been confirmed by an independent lattice calculation.

J.-S. Yoo, T. Bhattacharya, R. Gupta, S. Mondal, and B. Yoon, Phys. Rev. D 108, 034508 (2023).

Review of the Result of Pion Channel

北京大学 PEKING UNIVERSITY

➢Our calculation leads to a reduction of the total theoretical uncertainty from theory by a factor of 3.

$$|V_{ud}| = 0.9739(28)_{\mathrm{exp}}(5)_{\mathrm{th}} \rightarrow 0.9740(28)_{\mathrm{exp}}(1)_{\mathrm{th}}$$

Review of the Result of Pion Channel

北京大学 PEKING UNIVERSITY

- Our calculation leads to a reduction of the total theoretical uncertainty from theory by a factor of 3.

$$|V_{ud}| = 0.9739(28)_{\rm exp}(5)_{\rm th} \rightarrow 0.9740(28)_{\rm exp}(1)_{\rm th}$$

- PDG 2022 cites our calculation and look forward to improvement for experimental input.

> Theoretical uncertainties in pion beta decay are very small [21], leaving open more than an order of magnitude improvement of its experimental branching ratio before theory uncertainties become a problem. Although challenging, improved measurements of pion beta decay currently under discussion would allow this decay mode to compete with superallowed beta decays and future neutron decay efforts for the most precise direct $|V_{ud}|$ determination.

[21] X. Feng *et al.*, Phys. Rev. Lett. **124**, 19, 192002 (2020), [arXiv:2003.09798].

Review of the Result of Pion Channel

北京大学 PEKING UNIVERSITY

- Our calculation leads to a reduction of the total theoretical uncertainty from theory by a factor of 3.

$$|V_{ud}| = 0.9739(28)_{\rm exp}(5)_{\rm th} \rightarrow 0.9740(28)_{\rm exp}(1)_{\rm th}$$

- PDG 2022 cites our calculation and look forward to improvement for experimental input.

> Theoretical uncertainties in pion beta decay are very small [21], leaving open more than an order of magnitude improvement of its experimental branching ratio before theory uncertainties become a problem. Although challenging, improved measurements of pion beta decay currently under discussion would allow this decay mode to compete with superallowed beta decays and future neutron decay efforts for the most precise direct $|V_{ud}|$ determination.

[21] X. Feng *et al.*, Phys. Rev. Lett. **124**, 19, 192002 (2020), [arXiv:2003.09798].

Review of the Result of Pion Channel

北京大学 PEKING UNIVERSITY

➢Our calculation leads to a reduction of the total theoretical uncertainty from theory by a factor of 3.

$$|V_{ud}| = 0.9739(28)_{\rm exp}(5)_{\rm th} \to 0.9740(28)_{\rm exp}(1)_{\rm th}$$

➢PDG 2022 cites our calculation and look forward to improvement for experimental input.

Theoretical uncertainties in pion beta decay are very small [21], leaving open more than an order of magnitude improvement of its experimental branching ratio before theory uncertainties become a problem. Although challenging, improved measurements of pion beta decay currently under discussion would allow this decay mode to compete with superallowed beta decays and future neutron decay efforts for the most precise direct $|V_{ud}|$ determination.

[21] X. Feng *et al.*, Phys. Rev. Lett. **124**, 19, 192002 (2020), [arXiv:2003.09798].

➢The PIONEER experiment is aimed at improving the V_{ud} from pion beta decay at the 0.02% level.

up to the PeV mass scale. The later phases of the PIONEER experiment aim at improving the experimental precision of the branching ratio of pion beta decay, $\pi^+ \to \pi^0 e^+ \nu(\gamma)$, to test CKM unitarity and to extract $|V_{ud}|$ at the 0.02% level.

0.27% → 0.02%

Review of the Result of Pion Channel

北京大学 PEKING UNIVERSITY

➢Our calculation leads to a reduction of the total theoretical uncertainty from theory by a factor of 3.

$$|V_{ud}| = 0.9739(28)_{\text{exp}}(5)_{\text{th}} \rightarrow 0.9740(28)_{\text{exp}}(1)_{\text{th}}$$

➢PDG 2022 cites our calculation and look forward to improvement for experimental input.

Theoretical uncertainties in pion beta decay are very small [21], leaving open more than an order of magnitude improvement of its experimental branching ratio before theory uncertainties become a problem. Although challenging, improved measurements of pion beta decay currently under discussion would allow this decay mode to compete with superallowed beta decays and future neutron decay efforts for the most precise direct $|V_{ud}|$ determination.

[21] X. Feng *et al.*, Phys. Rev. Lett. **124**, 19, 192002 (2020), [arXiv:2003.09798].

➢The PIONEER experiment is aimed at improving the V_{ud} from pion beta decay at the 0.02% level.

up to the PeV mass scale. The later phases of the PIONEER experiment aim at improving the experimental precision of the branching ratio of pion beta decay, $\pi^+ \rightarrow \pi^0 e^+ \nu(\gamma)$, to test CKM unitarity and to extract $|V_{ud}|$ at the 0.02% level.

0.27% → 0.02%

➢ If the funding decisions are positive and proceed expeditiously, Phase I of PIONEER will begin in 2029.

More Contractions

More Contractions

- There are 4 types of contractions for meson channel:

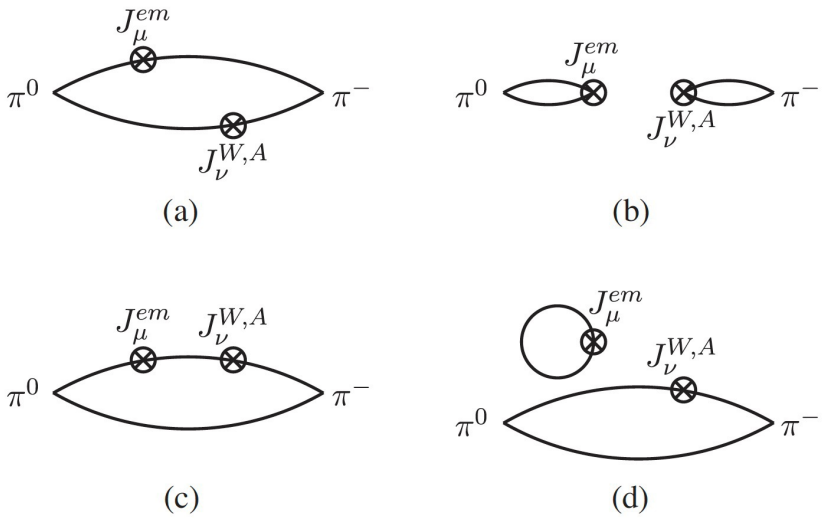

- For each type, the contraction for baryon is more complicated than meson.

- To solve this problem, we take the field-sparsening method*.

More Contractions

- There are 4 types of contractions for meson channel:

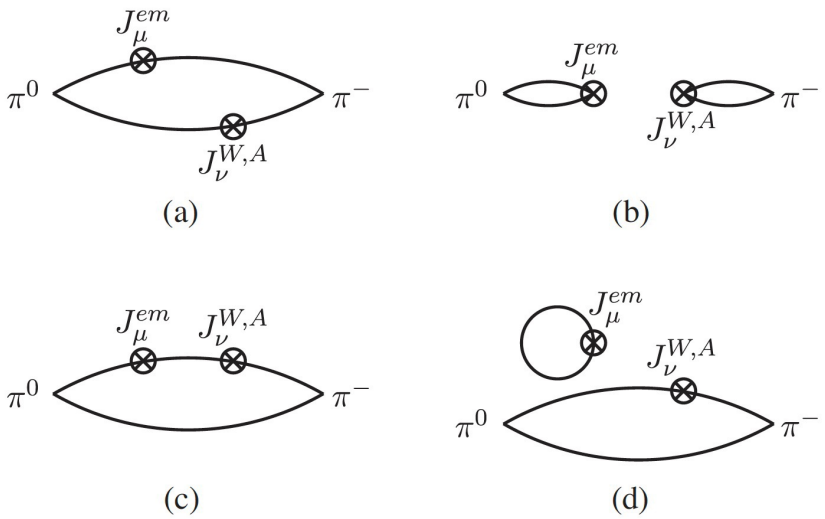

- For each type, the contraction for baryon is more complicated than meson.

- To solve this problem, we take the field-sparsening method*.

- While for baryon channel, there are 10 types:

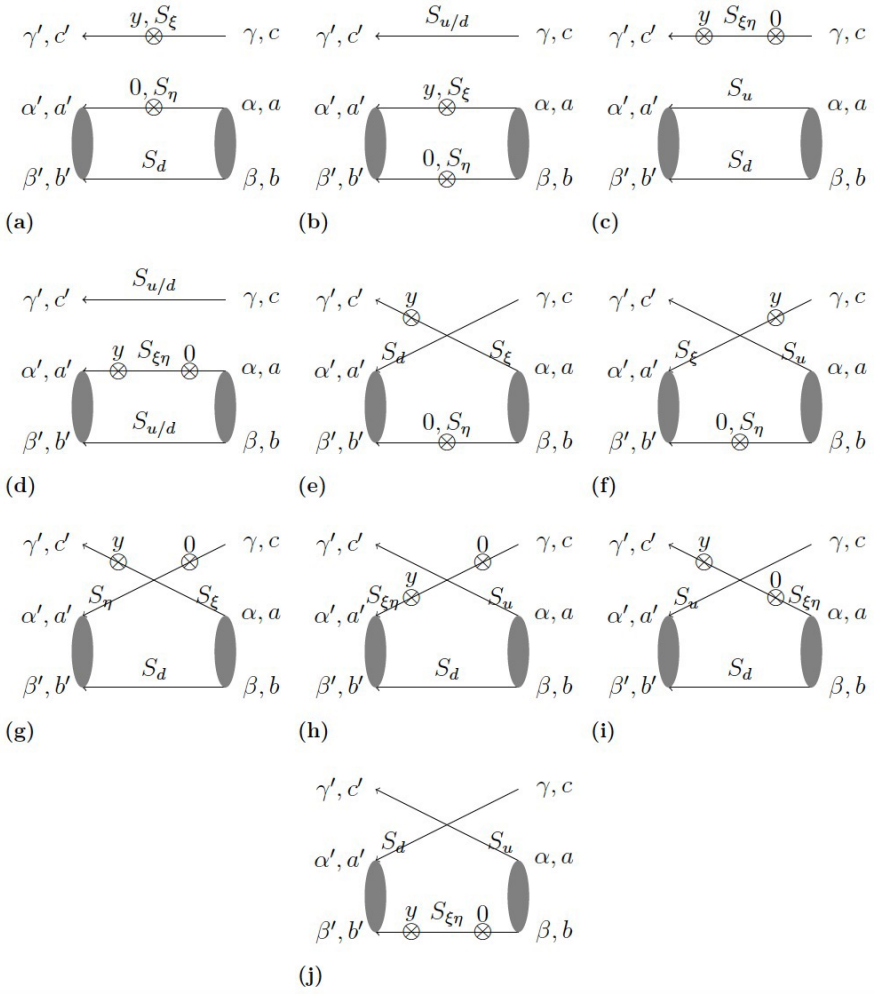

More Contractions

- There are 4 types of contractions for meson channel:

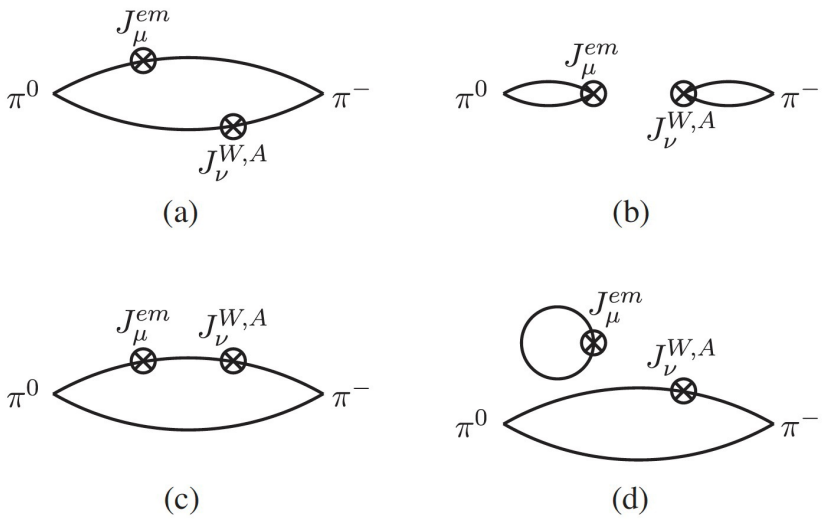

- For each type, the contraction for baryon is more complicated than meson.

- To solve this problem, we take the field-sparsening method*.

- While for baryon channel, there are 10 types:

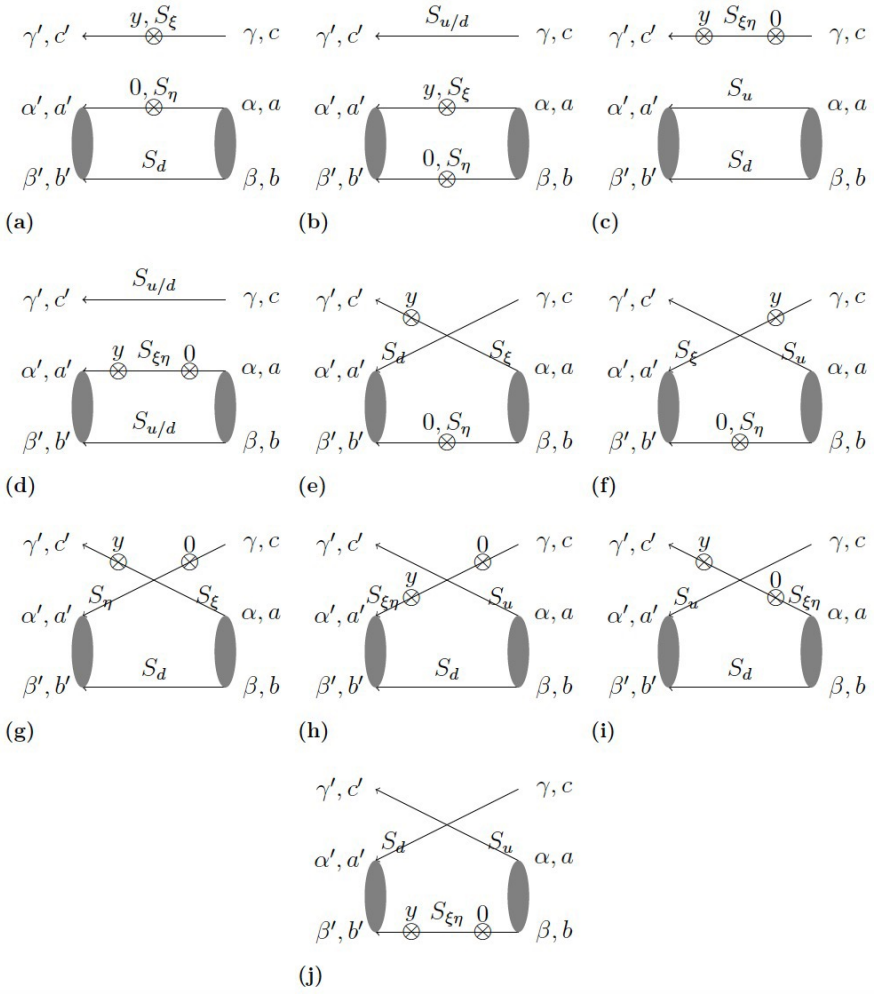

More Contractions

- There are 4 types of contractions for meson channel:

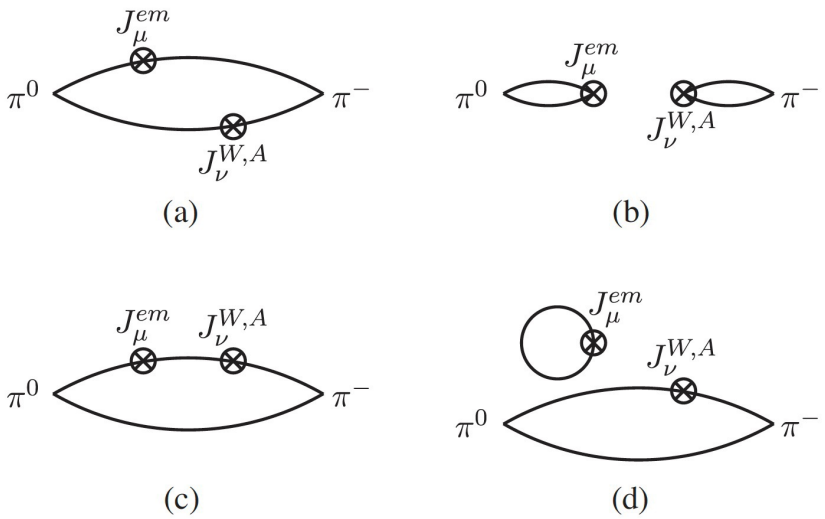

- For each type, the contraction for baryon is more complicated than meson.

- To solve this problem, we take the field-sparsening method*.

*: Y. Li, S. C. Xia, X. Feng, L. C. Jin and C. Liu, Phys. Rev. D 103, no.1, 014514 (2021).

- While for baryon channel, there are 10 types:

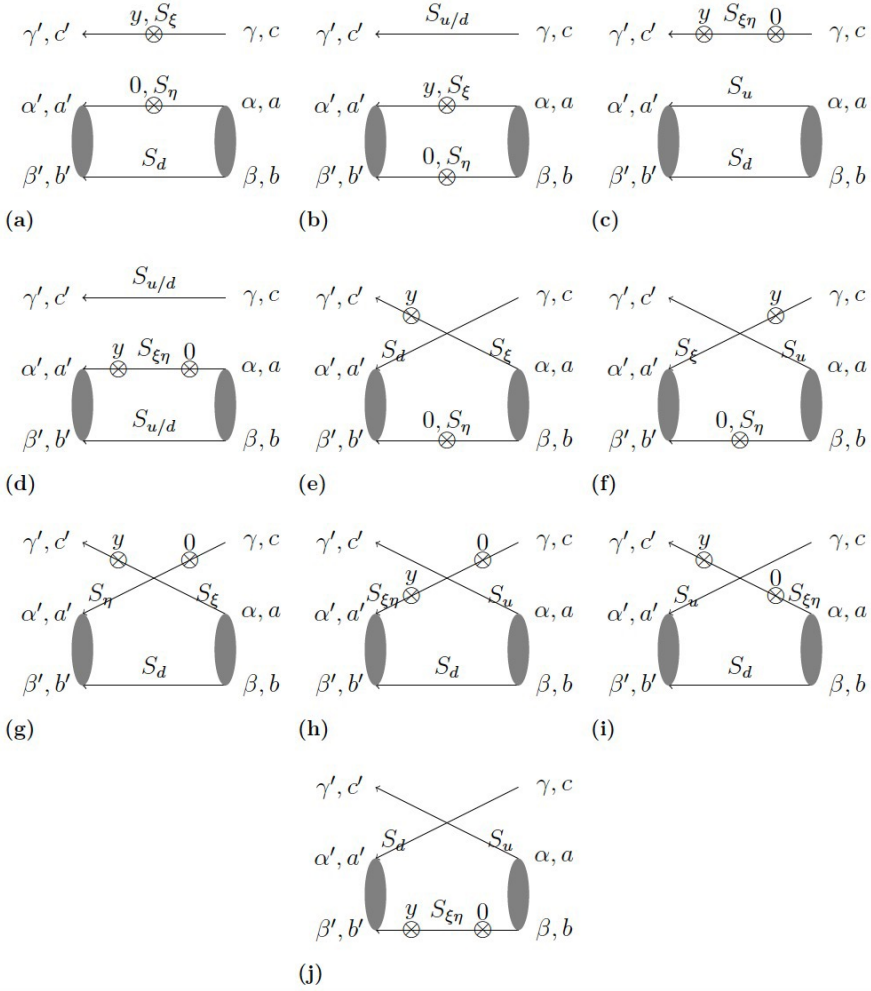

More Contractions

- There are 4 types of contractions for meson channel:

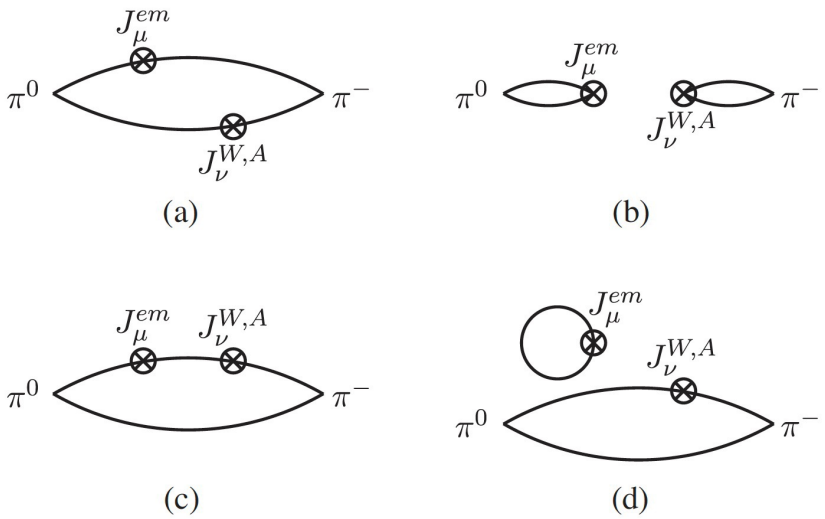

- While for baryon channel, there are 10 types:

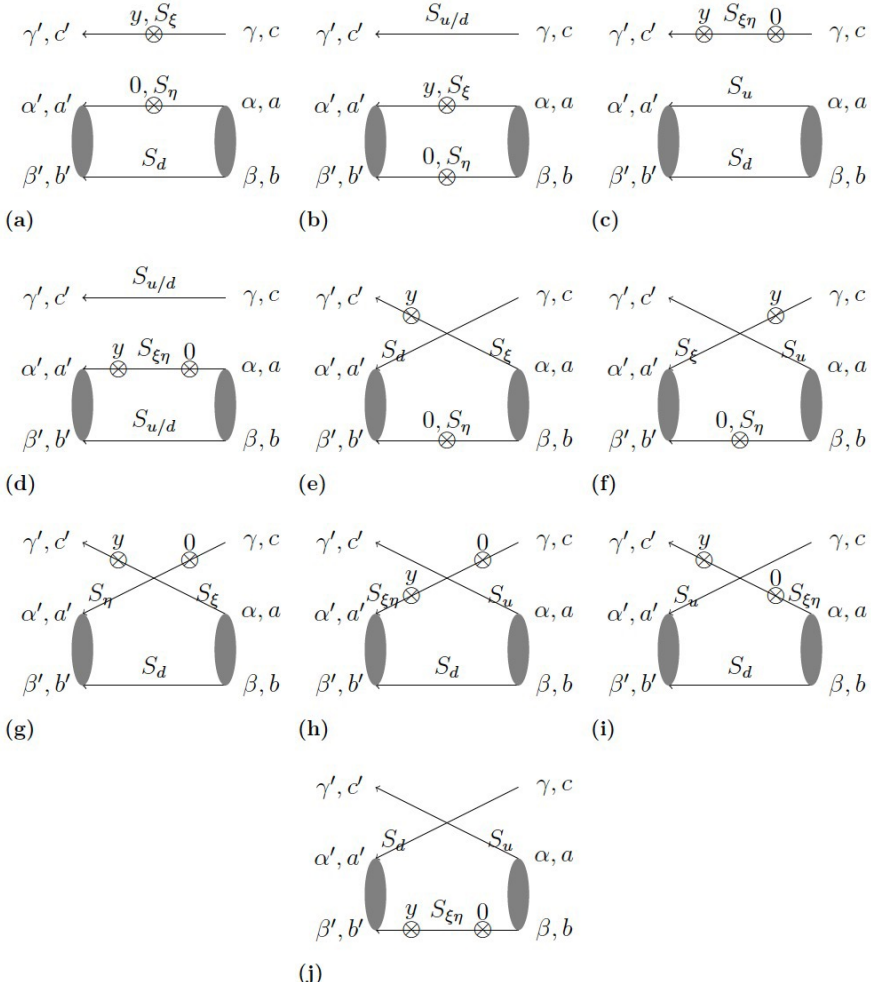

- For each type, the contraction for baryon is more complicated than meson.

- To solve this problem, we take the field-sparsening method*.

*: Y. Li, S. C. Xia, X. Feng, L. C. Jin and C. Liu, Phys. Rev. D 103, no.1, 014514 (2021).

- The computational cost has been reduced by a factor of 10^3, while the precision remains nearly unchanged.

Signal-to-Noise Problem

北京大学
PEKING UNIVERSITY

Signal-to-Noise Problem

- The variance of a physical quantity is associated with its square's expectation.
- The signal-to-noise of π's two-point function is under good control:

$$\mathrm{E}(\pi) \sim e^{-m_\pi t}$$

$$\mathrm{Var}(\pi) \sim e^{-2m_\pi t}$$

- In noise of neutron's two-point function, the simplest structure is three-π:

- For physical ensembles, as T becomes larger, the data from neutron will be too noise to be used.

Signal-to-Noise Problem

- The variance of a physical quantity is associated with its square's expectation.
- The signal-to-noise of π's two-point function is under good control:

$$\mathrm{E}(\pi) \sim e^{-m_\pi t}$$

$$\mathrm{Var}(\pi) \sim e^{-2m_\pi t}$$

- In noise of neutron's two-point function, the simplest structure is three-π:

- For physical ensembles, as T becomes larger, the data from neutron will be too noise to be used.

Signal-to-Noise Problem

- The variance of a physical quantity is associated with its square's expectation.
- The signal-to-noise of π's two-point function is under good control:

$$\mathrm{E}(\pi) \sim e^{-m_\pi t}$$

$$\mathrm{Var}(\pi) \sim e^{-2m_\pi t}$$

- In noise of neutron's two-point function, the simplest structure is three-π:

$$\mathrm{E}(n) \sim e^{-m_n t}$$

$$\mathrm{Var}(n) \sim e^{-3m_\pi t}$$

- For physical ensembles, as T becomes larger, the data from neutron will be too noise to be used.

Signal-to-Noise Problem

北京大学 PEKING UNIVERSITY

- The variance of a physical quantity is associated with its square's expectation.
- The signal-to-noise of π's two-point function is under good control:

$$\mathrm{E}(\pi) \sim e^{-m_\pi t}$$

$$\mathrm{Var}(\pi) \sim e^{-2m_\pi t}$$

- In noise of neutron's two-point function, the simplest structure is three-π:

$$\mathrm{E}(\mathrm{n}) \sim e^{-m_n t}$$

$$\mathrm{Var}(\mathrm{n}) \sim e^{-3m_\pi t}$$

- For physical ensembles, $m_n > \frac{3}{2} m_\pi$, as T becomes larger, the data from neutron will be too noise to be used.

Convergence of Temporal Integration

- Baryon has different spin structure from meson, so they have different intermediate state:

- The spatial component for axial current has even parity, so:

Convergence of Temporal Integration

- Baryon has different spin structure from meson, so they have different intermediate state:

- The spatial component for axial current has even parity, so:

$$\langle \pi | J^{\mu}_{W,A} | \pi \rangle = 0$$

Convergence of Temporal Integration

- Baryon has different spin structure from meson, so they have different intermediate state:

- The spatial component for axial current has even parity, so:

$$\langle \pi | J^{\mu}_{W,A} | \pi \rangle = 0$$

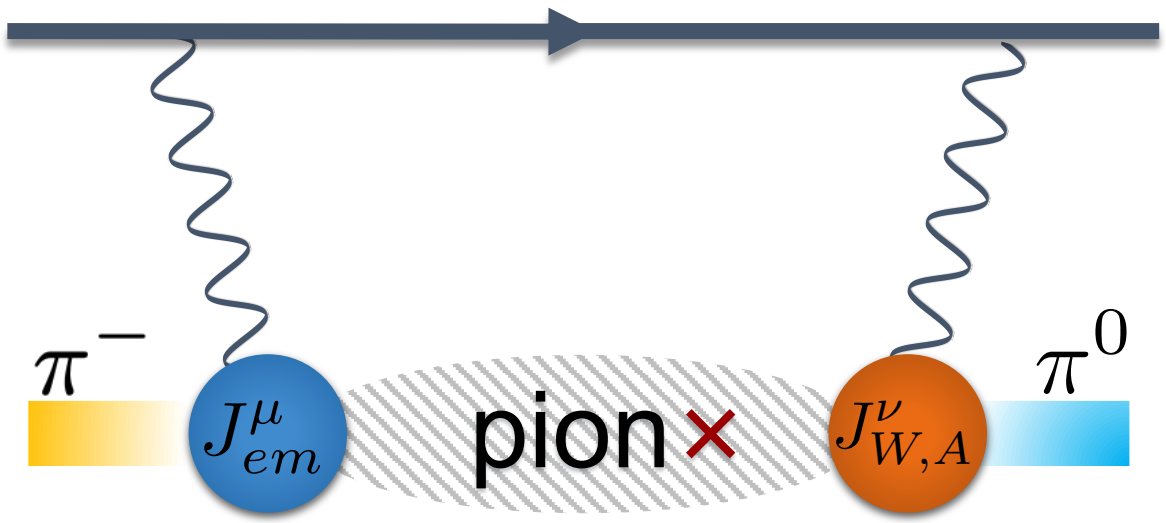

Convergence of Temporal Integration

- Baryon has different spin structure from meson, so they have different intermediate state:

- The spatial component for axial current has even parity, so:

$$\langle \pi | J^{\mu}_{W,A} | \pi \rangle = 0$$

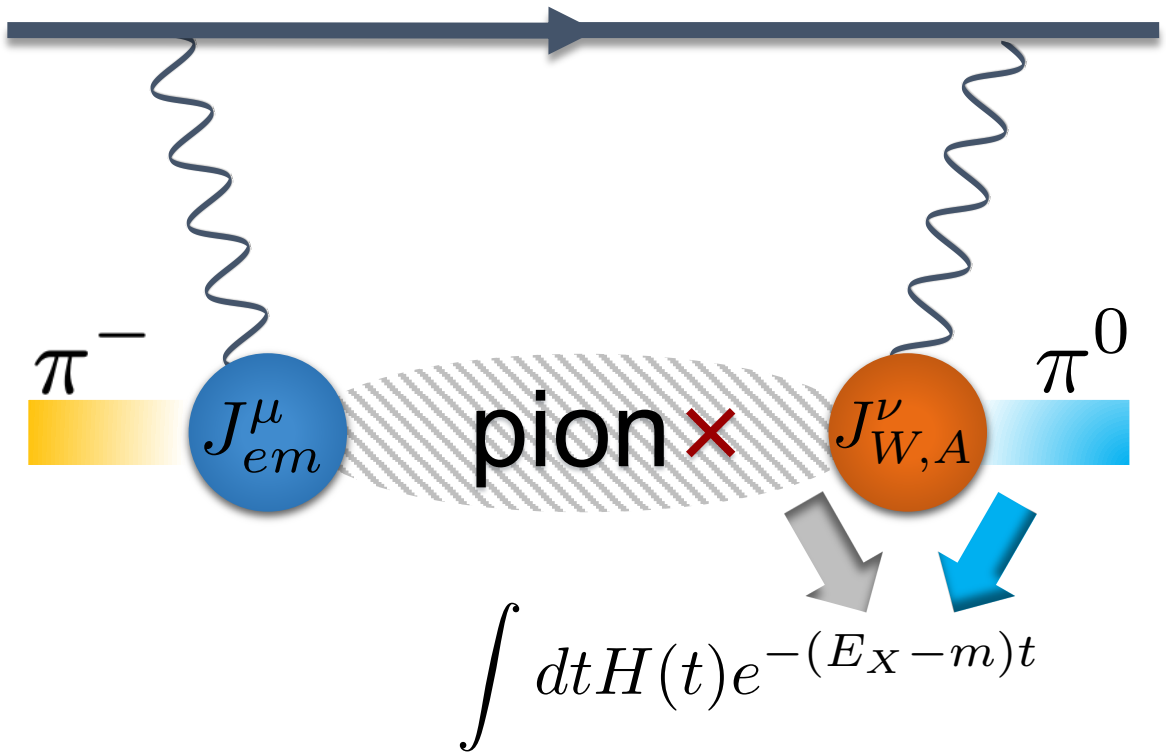

Convergence of Temporal Integration

- Baryon has different spin structure from meson, so they have different intermediate state:

- The spatial component for axial current has even parity, so:

$$\langle \pi | J^{\mu}_{W,A} | \pi \rangle = 0$$

$$\langle n | J^{\mu}_{W,A} | p \rangle \neq 0$$

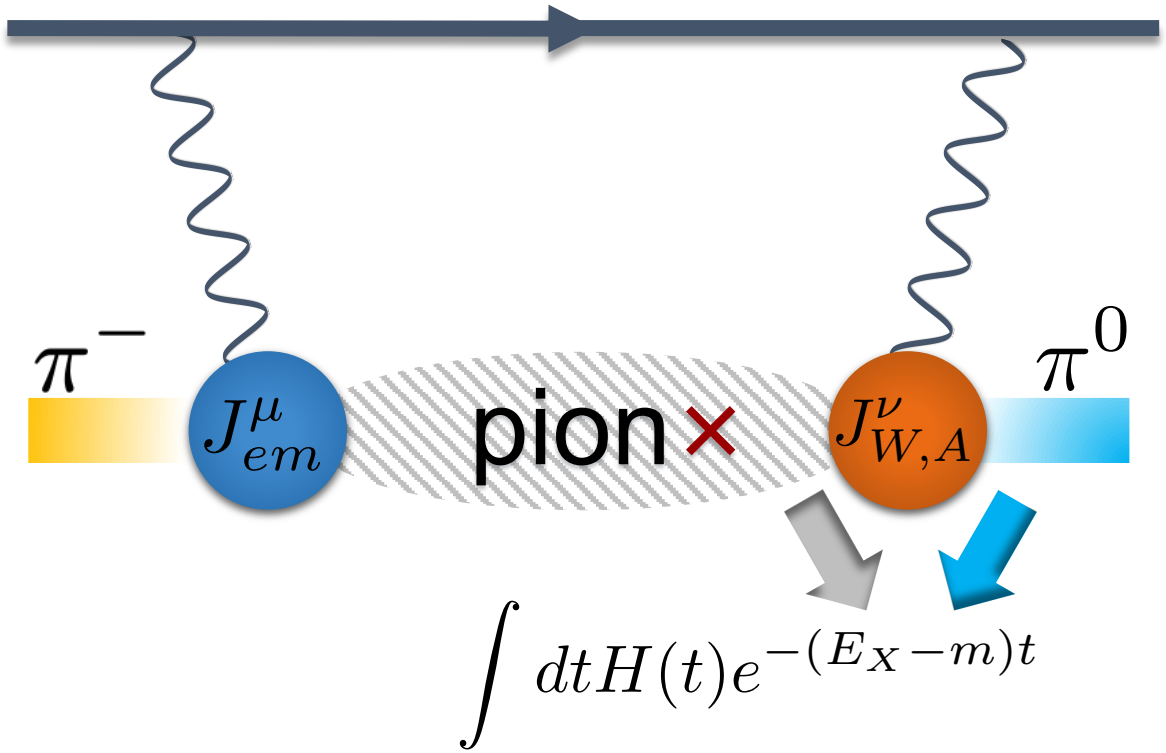

Convergence of Temporal Integration

北京大学 PEKING UNIVERSITY

- Baryon has different spin structure from meson, so they have different intermediate state:

- The spatial component for axial current has even parity, so:

$$\langle \pi | J^{\mu}_{W,A} | \pi \rangle = 0$$

$$\langle n | J^{\mu}_{W,A} | p \rangle \neq 0$$

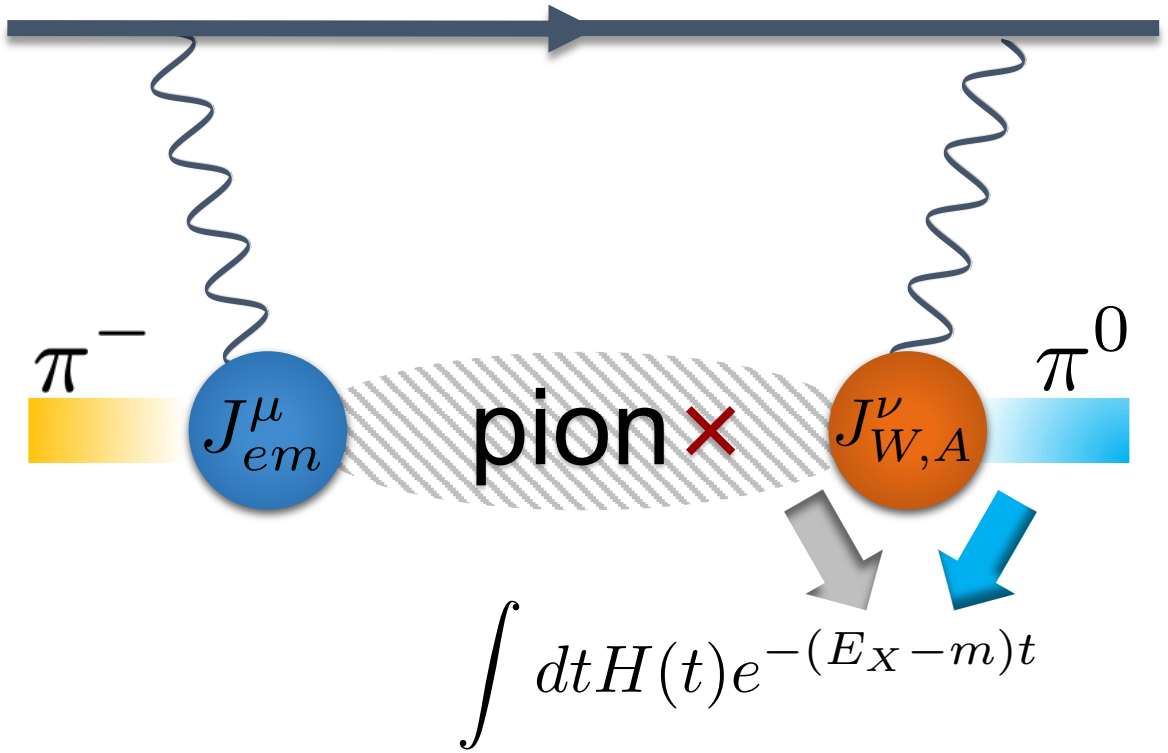

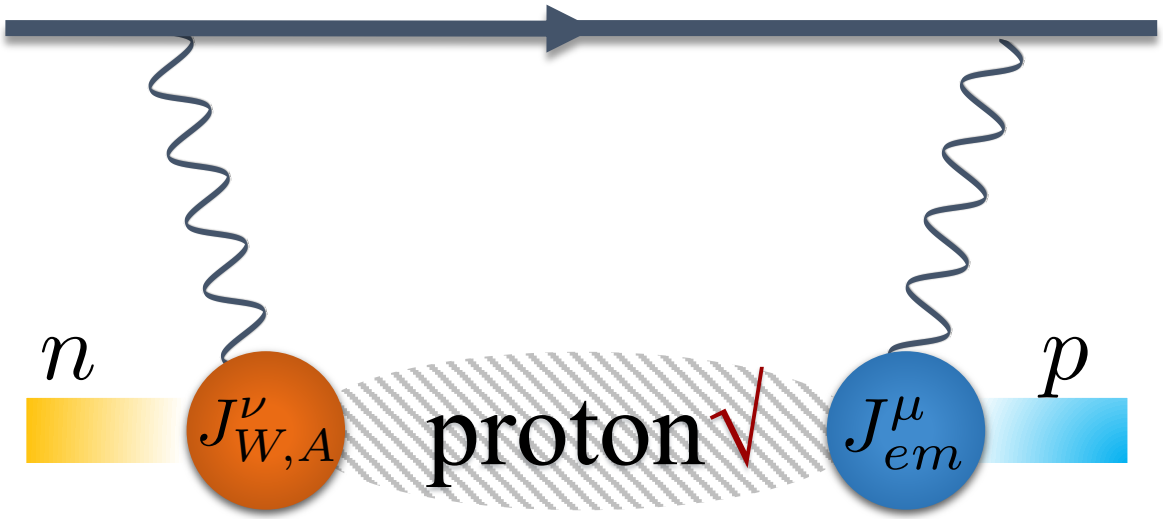

Convergence of Temporal Integration

- Baryon has different spin structure from meson, so they have different intermediate state:

- The spatial component for axial current has even parity, so:

$$\langle \pi | J^{\mu}_{W,A} | \pi \rangle = 0$$

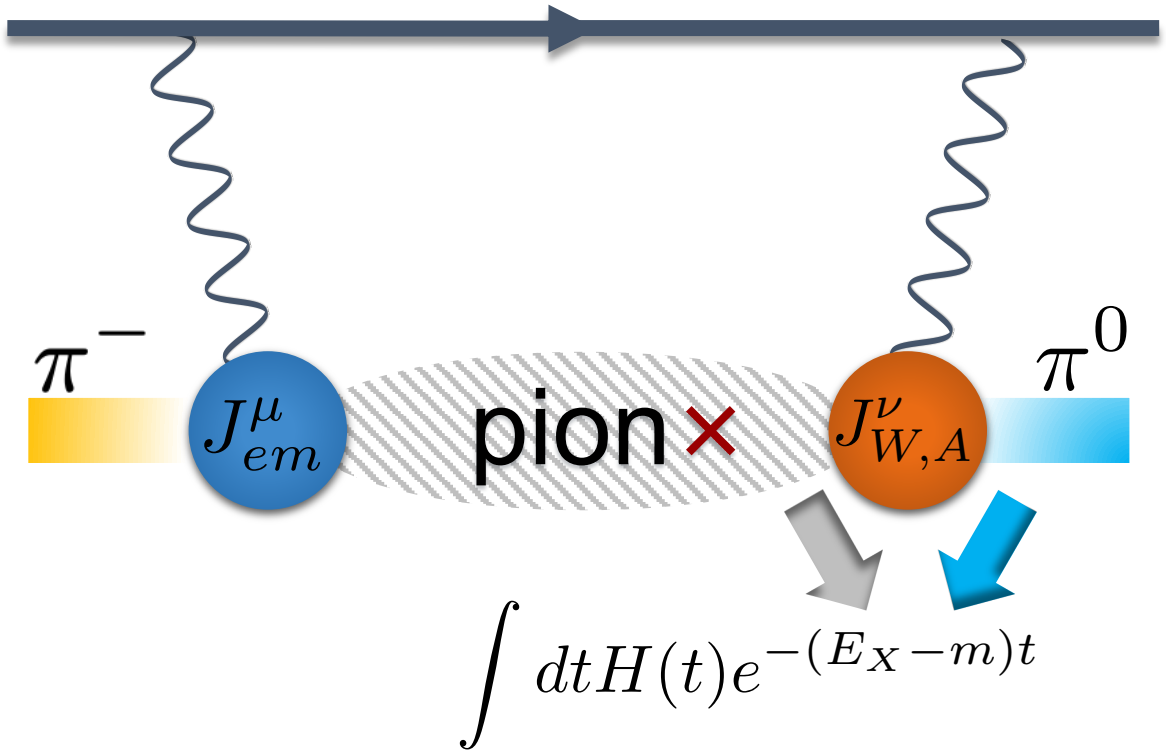

$$\langle n | J^{\mu}_{W,A} | p \rangle \neq 0$$

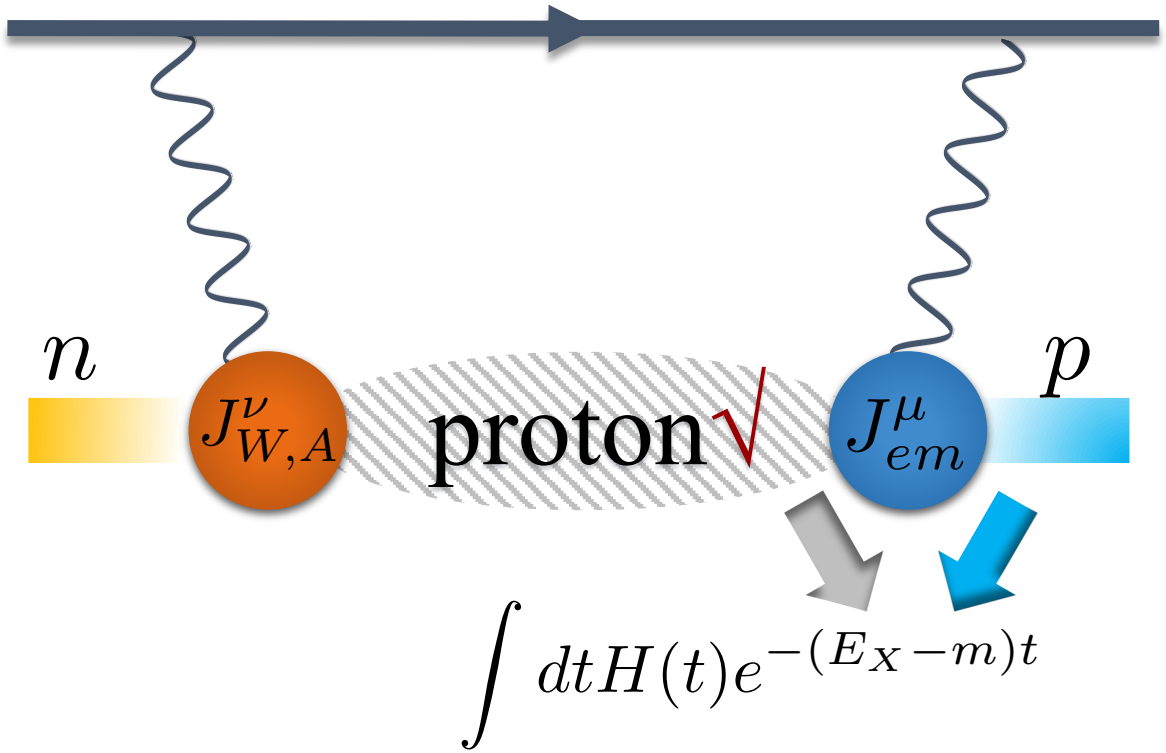

Convergence of Temporal Integration

北京大学 PEKING UNIVERSITY

- To solve the signal-to-noise problem and improve the convergence of temporal integration., we use the infinite volume reconstruction (IVR)* method.

X. Feng and L. Jin, Phys. Rev. D 100, no.9, 094509 (2019).

Convergence of Temporal Integration

北京大学 PEKING UNIVERSITY

- To solve the signal-to-noise problem and improve the convergence of temporal integration., we use the infinite volume reconstruction (IVR)* method.

X. Feng and L. Jin, Phys. Rev. D 100, no.9, 094509 (2019).

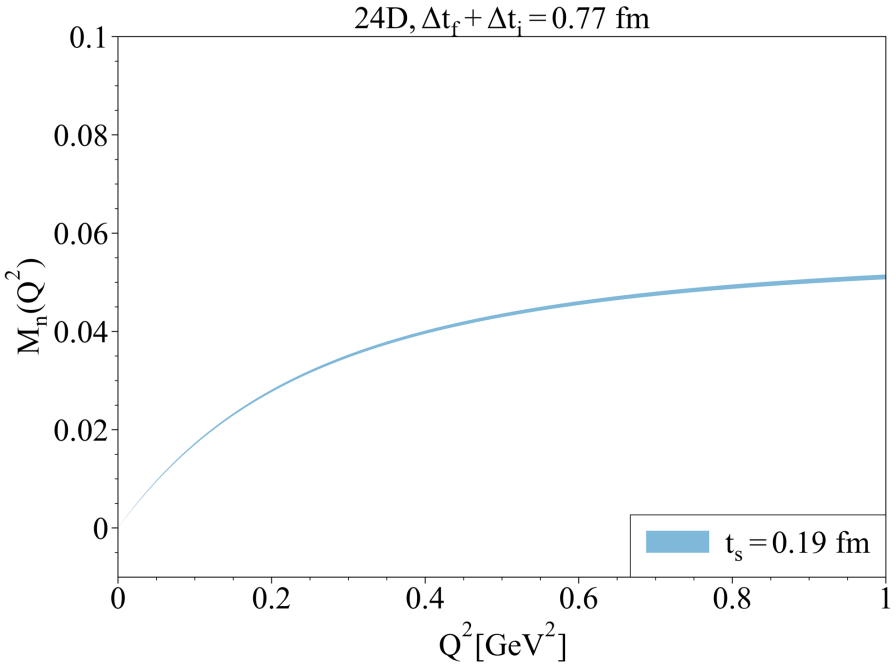

Convergence of Temporal Integration

北京大学 PEKING UNIVERSITY

- To solve the signal-to-noise problem and improve the convergence of temporal integration., we use the infinite volume reconstruction (IVR)* method.

X. Feng and L. Jin, Phys. Rev. D 100, no.9, 094509 (2019).

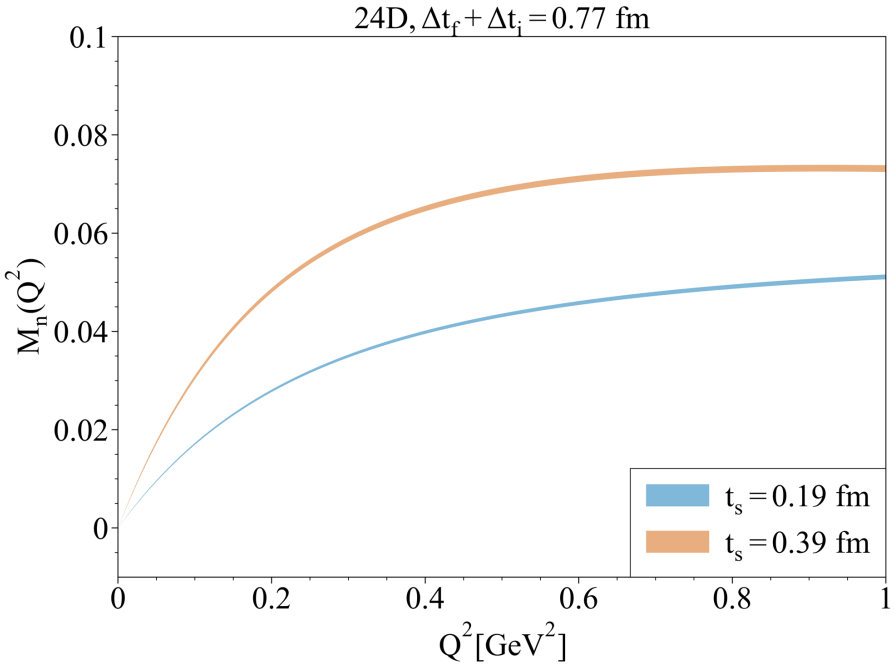

Convergence of Temporal Integration

北京大学 PEKING UNIVERSITY

- To solve the signal-to-noise problem and improve the convergence of temporal integration., we use the infinite volume reconstruction (IVR)* method.

X. Feng and L. Jin, Phys. Rev. D 100, no.9, 094509 (2019).

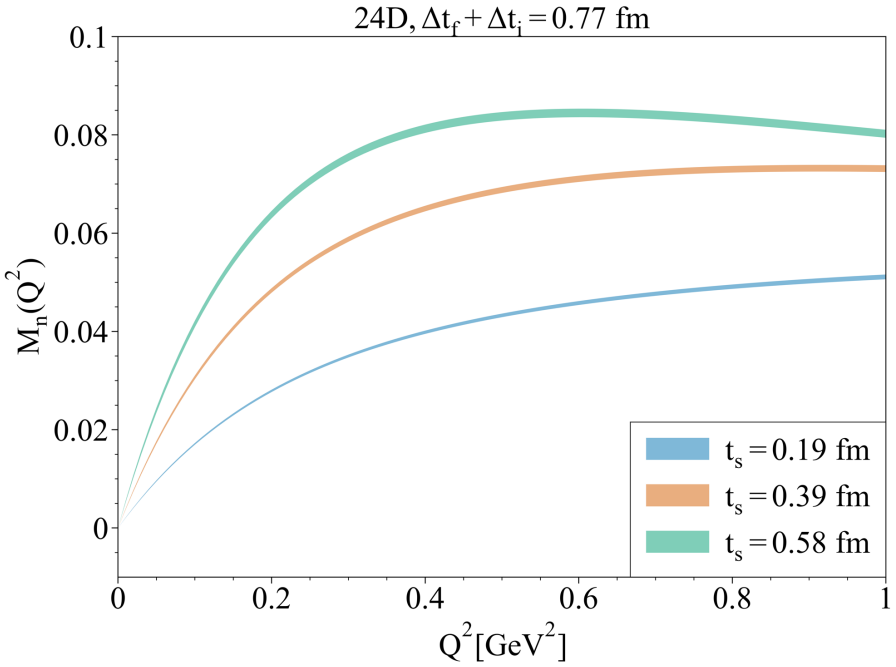

Convergence of Temporal Integration

北京大学 PEKING UNIVERSITY

- To solve the signal-to-noise problem and improve the convergence of temporal integration., we use the infinite volume reconstruction (IVR)* method.

X. Feng and L. Jin, Phys. Rev. D 100, no.9, 094509 (2019).

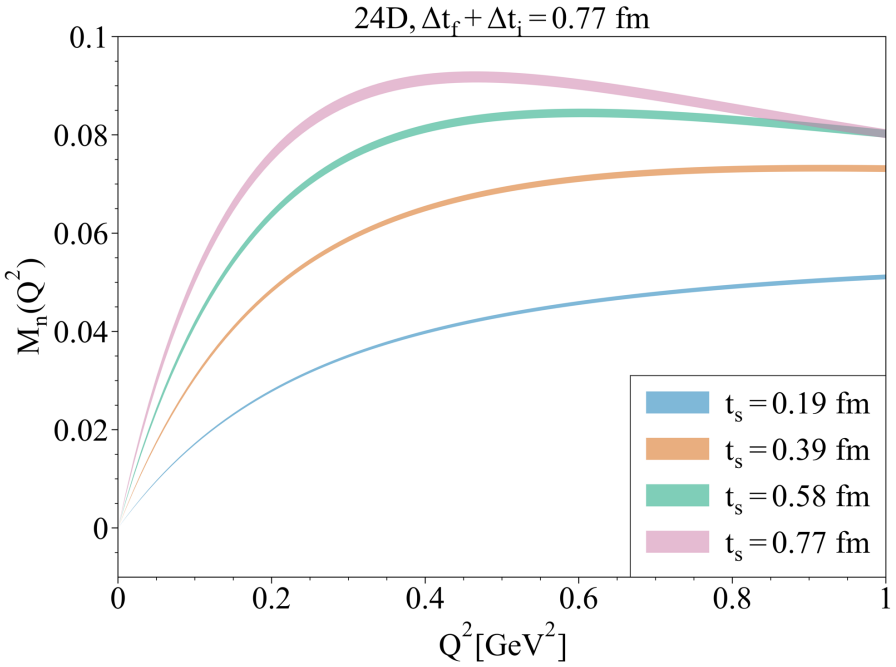

Convergence of Temporal Integration

北京大学 PEKING UNIVERSITY

- To solve the signal-to-noise problem and improve the convergence of temporal integration., we use the infinite volume reconstruction (IVR)* method.

X. Feng and L. Jin, Phys. Rev. D 100, no.9, 094509 (2019).

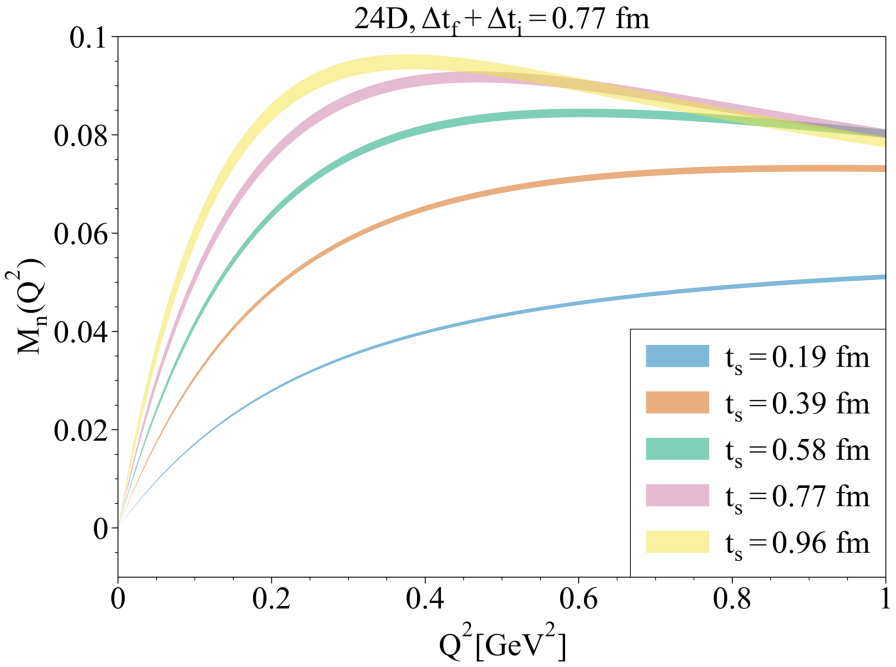

Convergence of Temporal Integration

北京大学 PEKING UNIVERSITY

- To solve the signal-to-noise problem and improve the convergence of temporal integration., we use the infinite volume reconstruction (IVR)* method.

X. Feng and L. Jin, Phys. Rev. D 100, no.9, 094509 (2019).

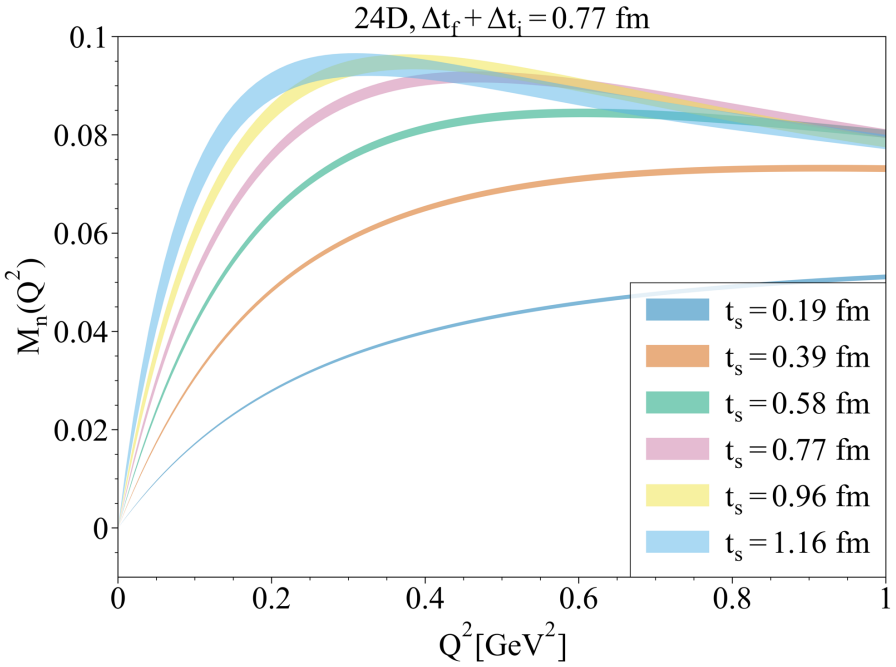

Convergence of Temporal Integration

北京大学 PEKING UNIVERSITY

- To solve the signal-to-noise problem and improve the convergence of temporal integration., we use the infinite volume reconstruction (IVR)* method.

X. Feng and L. Jin, Phys. Rev. D 100, no.9, 094509 (2019).

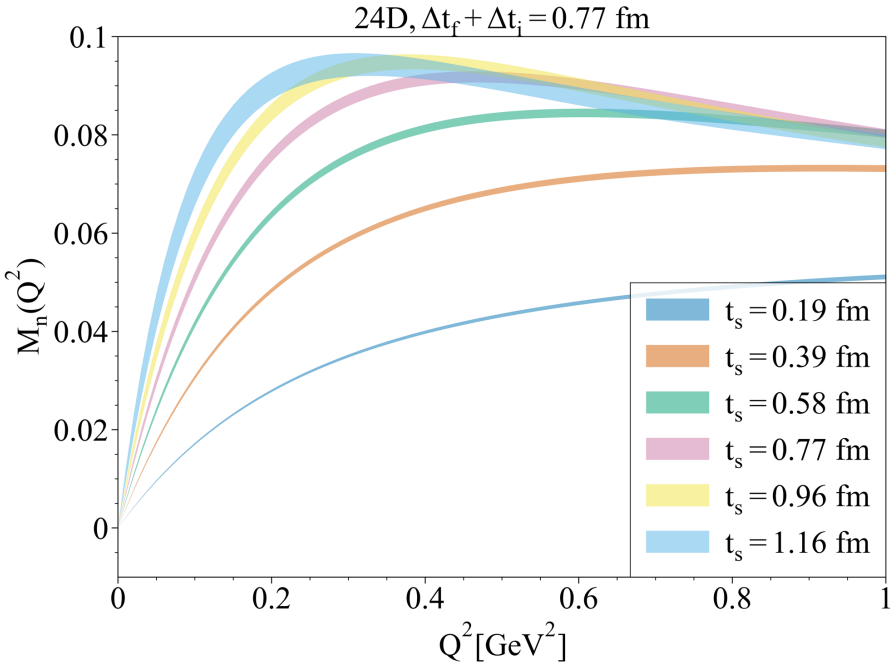

T = 1.16 fm is enough?

Convergence of Temporal Integration

北京大学 PEKING UNIVERSITY

- To solve the signal-to-noise problem and improve the convergence of temporal integration., we use the infinite volume reconstruction (IVR)* method.

X. Feng and L. Jin, Phys. Rev. D 100, no.9, 094509 (2019).

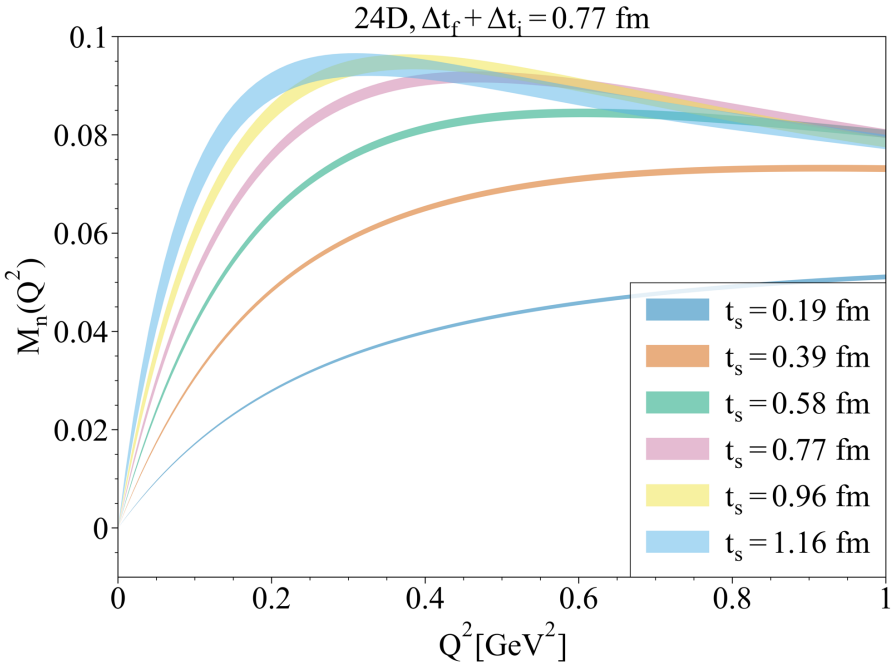

T = 1.16 fm is enough?

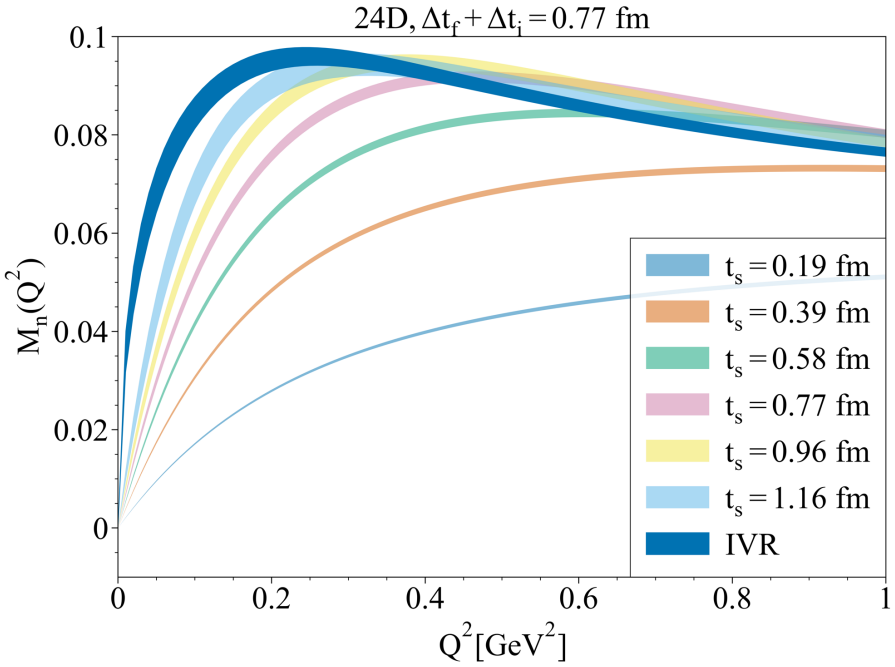

Infinite Volume Reconstruction

$$M_n^{\mathrm{SD}}\left(Q^2,t_s\right)=-\frac{1}{6}\frac{\sqrt{Q^2}}{m_N}\int_{-t_s}^{t_s}dt\int d^3\vec{x}\omega(t,\vec{x})H(t,\vec{x}),\qquad M_n^{\mathrm{LD}}\left(Q^2,t_s,t_g\right)=-\frac{1}{6}\frac{\sqrt{Q^2}}{m_N}\int d^3\vec{x}\tilde{\omega}\left(t_s,t_g,\vec{x}\right)\bar{H}\left(t_g,\vec{x}\right),$$

Short Distance (SD)

Long Distance (LD)

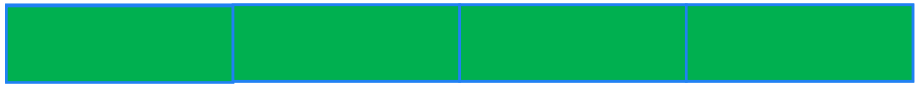

Infinite Volume Reconstruction

$$M_n^{\mathrm{SD}}\left(Q^2,t_s\right)=-\frac{1}{6}\frac{\sqrt{Q^2}}{m_N}\int_{-t_s}^{t_s}dt\int d^3\vec{x}\omega(t,\vec{x})H(t,\vec{x}),$$

$$M_n^{\mathrm{LD}}\left(Q^2,t_s,t_g\right)=-\frac{1}{6}\frac{\sqrt{Q^2}}{m_N}\int d^3\vec{x}\tilde{\omega}\left(t_s,t_g,\vec{x}\right)\bar{H}\left(t_g,\vec{x}\right),$$

Short Distance (SD)

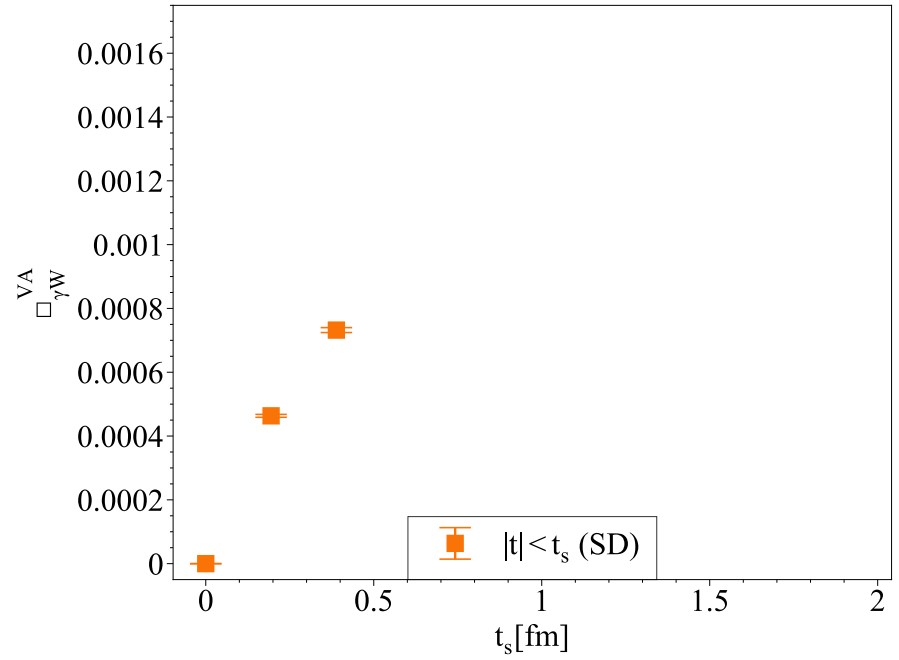

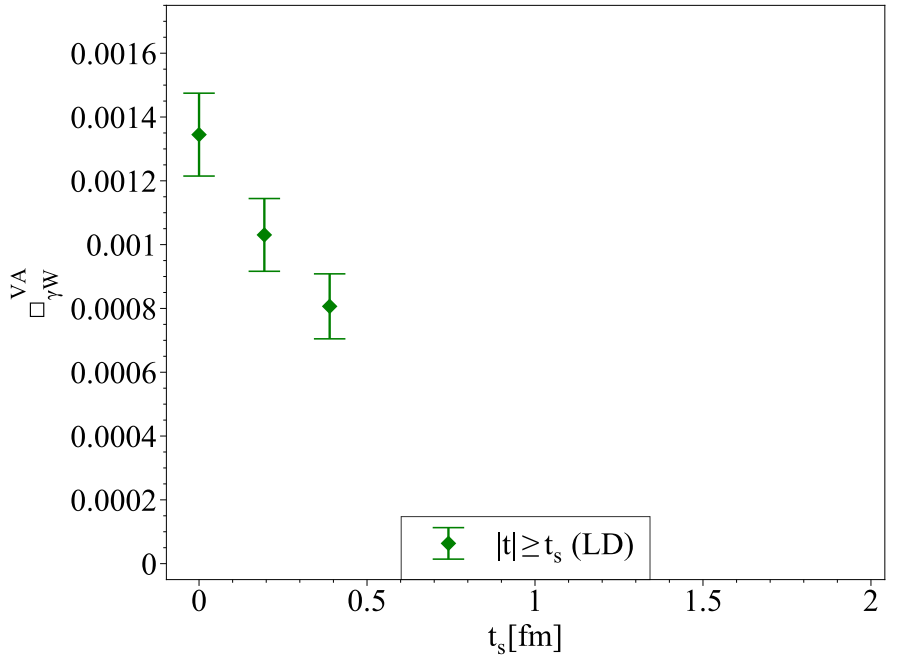

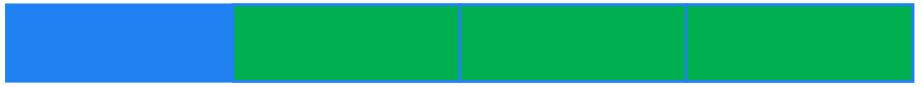

Long Distance (LD)

Infinite Volume Reconstruction

$$M_n^{\mathrm{SD}}\left(Q^2,t_s\right)=-\frac{1}{6}\frac{\sqrt{Q^2}}{m_N}\int_{-t_s}^{t_s}dt\int d^3\vec{x}\omega(t,\vec{x})H(t,\vec{x}),$$

$$M_n^{\mathrm{LD}}\left(Q^2,t_s,t_g\right)=-\frac{1}{6}\frac{\sqrt{Q^2}}{m_N}\int d^3\vec{x}\tilde{\omega}\left(t_s,t_g,\vec{x}\right)\bar{H}\left(t_g,\vec{x}\right),$$

Short Distance (SD)

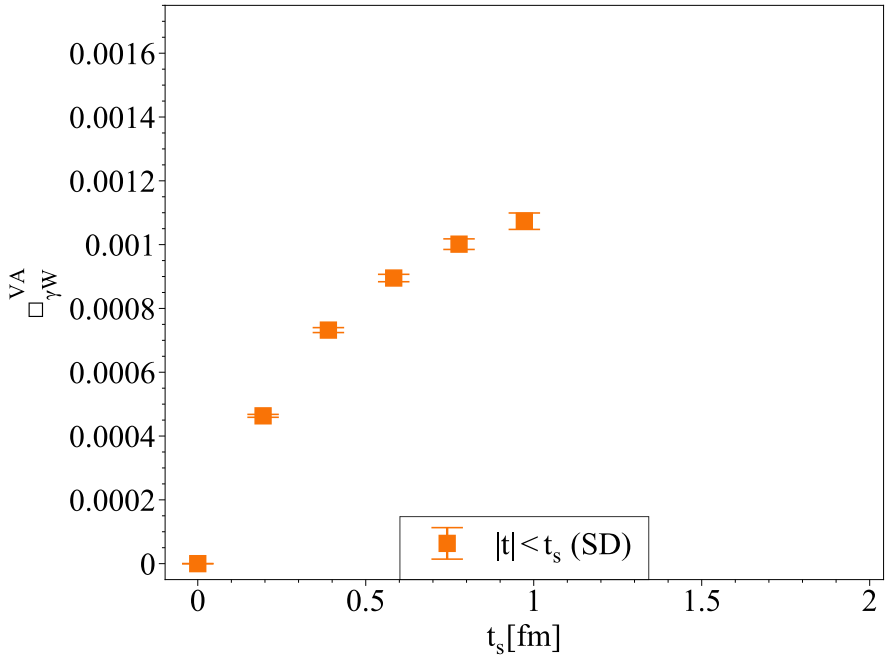

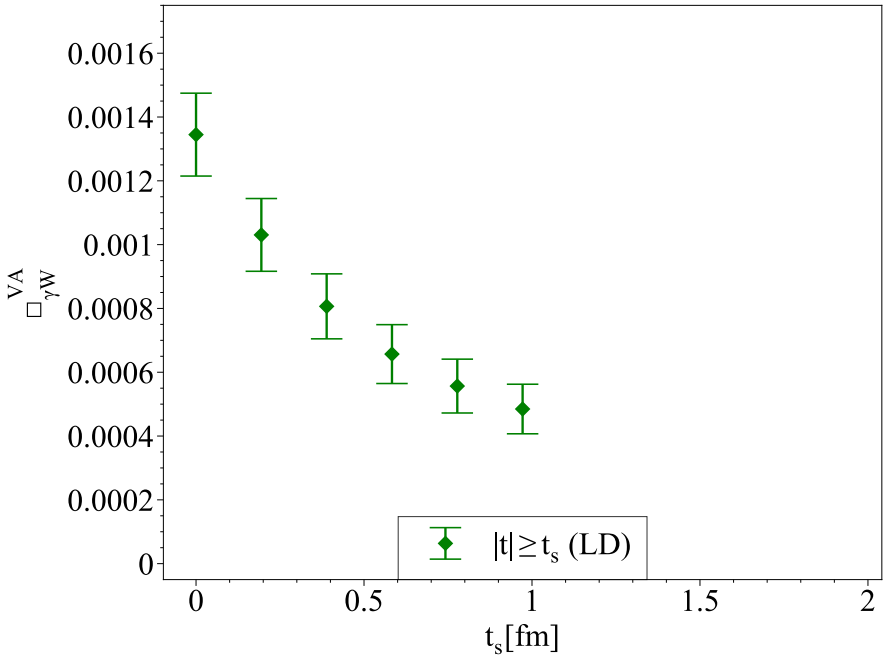

Long Distance (LD)

Infinite Volume Reconstruction

$$M_n^{\mathrm{SD}}\left(Q^2, t_s\right) = -\frac{1}{6}\frac{\sqrt{Q^2}}{m_N}\int_{-t_s}^{t_s} dt \int d^3\vec{x}\omega(t,\vec{x})H(t,\vec{x}),$$

$$M_n^{\mathrm{LD}}\left(Q^2, t_s, t_g\right) = -\frac{1}{6}\frac{\sqrt{Q^2}}{m_N}\int d^3\vec{x}\tilde{\omega}\left(t_s, t_g, \vec{x}\right)\bar{H}\left(t_g, \vec{x}\right),$$

Short Distance (SD)

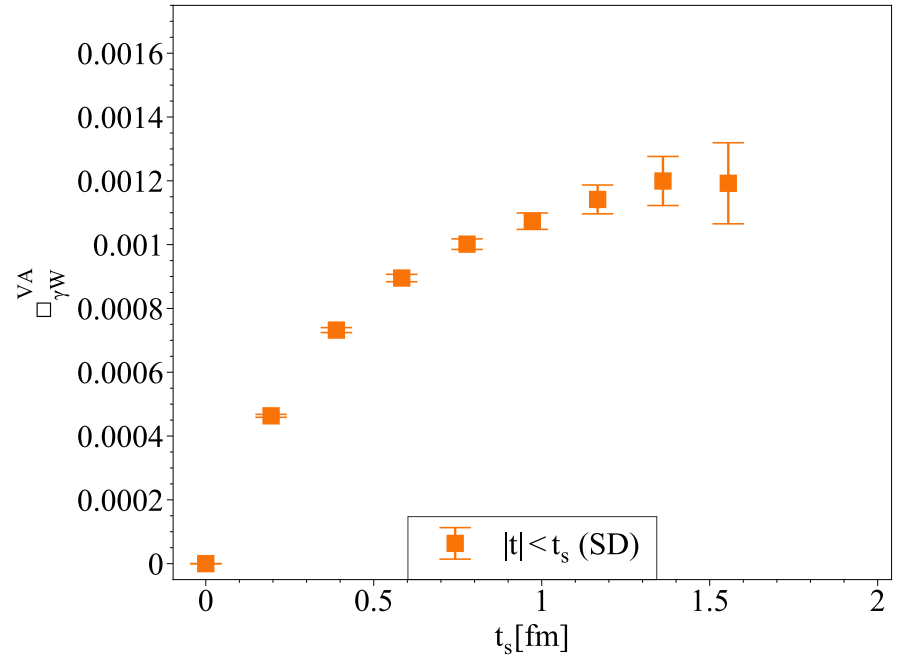

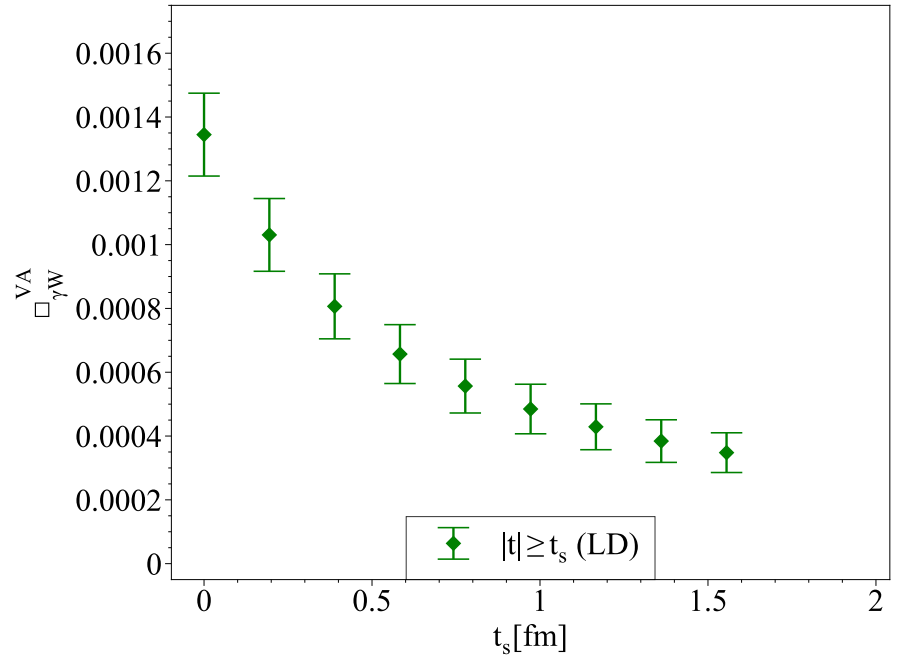

Long Distance (LD)

Infinite Volume Reconstruction

$$M_n^{\mathrm{SD}}\left(Q^2,t_s\right)=-\frac{1}{6}\frac{\sqrt{Q^2}}{m_N}\int_{-t_s}^{t_s}dt\int d^3\vec{x}\omega(t,\vec{x})H(t,\vec{x}),$$

$$M_n^{\mathrm{LD}}\left(Q^2,t_s,t_g\right)=-\frac{1}{6}\frac{\sqrt{Q^2}}{m_N}\int d^3\vec{x}\tilde{\omega}\left(t_s,t_g,\vec{x}\right)\bar{H}\left(t_g,\vec{x}\right),$$

Short Distance (SD)

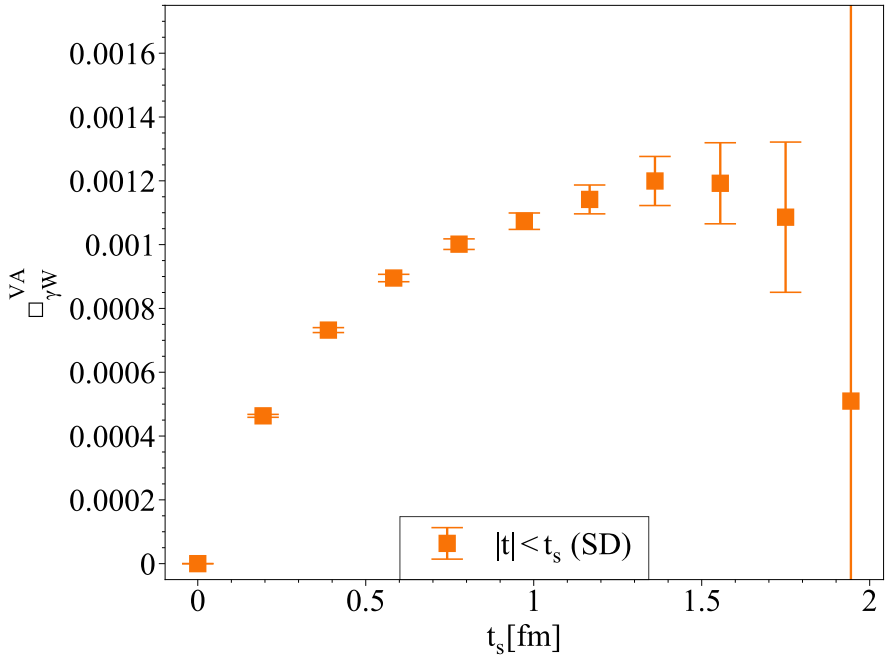

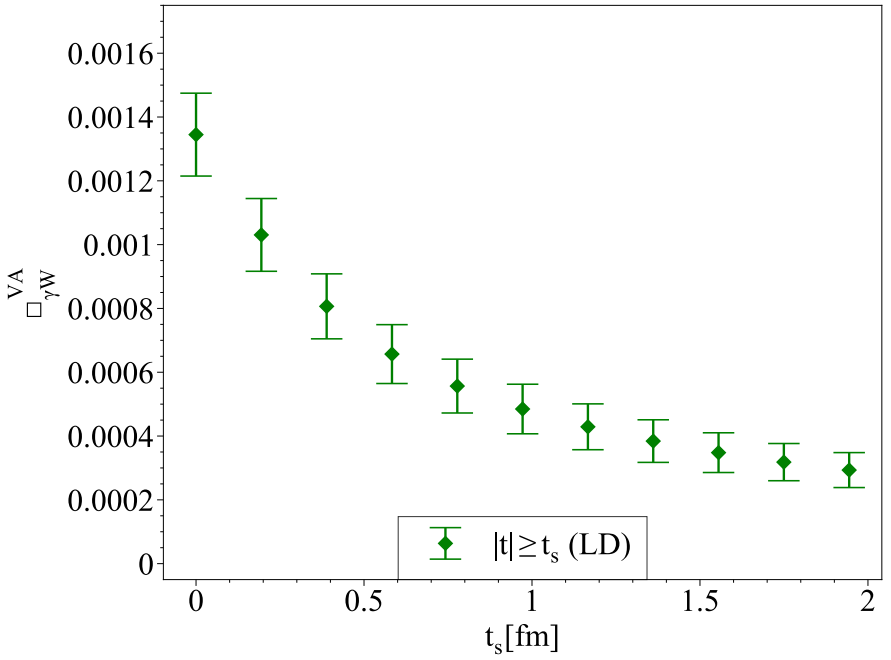

Long Distance (LD)

Infinite Volume Reconstruction

$$M_n^{\mathrm{SD}}\left(Q^2,t_s\right)=-\frac{1}{6}\frac{\sqrt{Q^2}}{m_N}\int_{-t_s}^{t_s}dt\int d^3\vec{x}\omega(t,\vec{x})H(t,\vec{x}),\qquad M_n^{\mathrm{LD}}\left(Q^2,t_s,t_g\right)=-\frac{1}{6}\frac{\sqrt{Q^2}}{m_N}\int d^3\vec{x}\tilde{\omega}\left(t_s,t_g,\vec{x}\right)\bar{H}\left(t_g,\vec{x}\right),$$

Short Distance (SD)

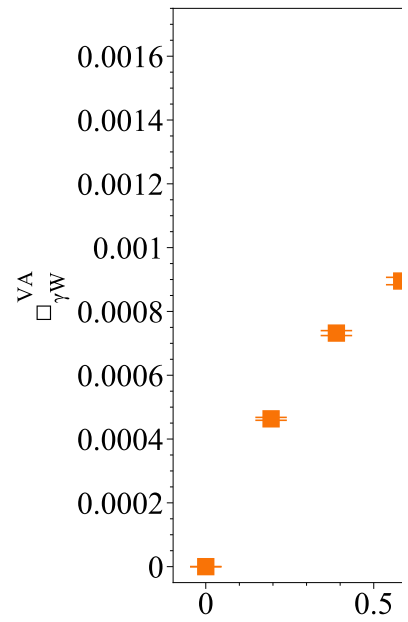

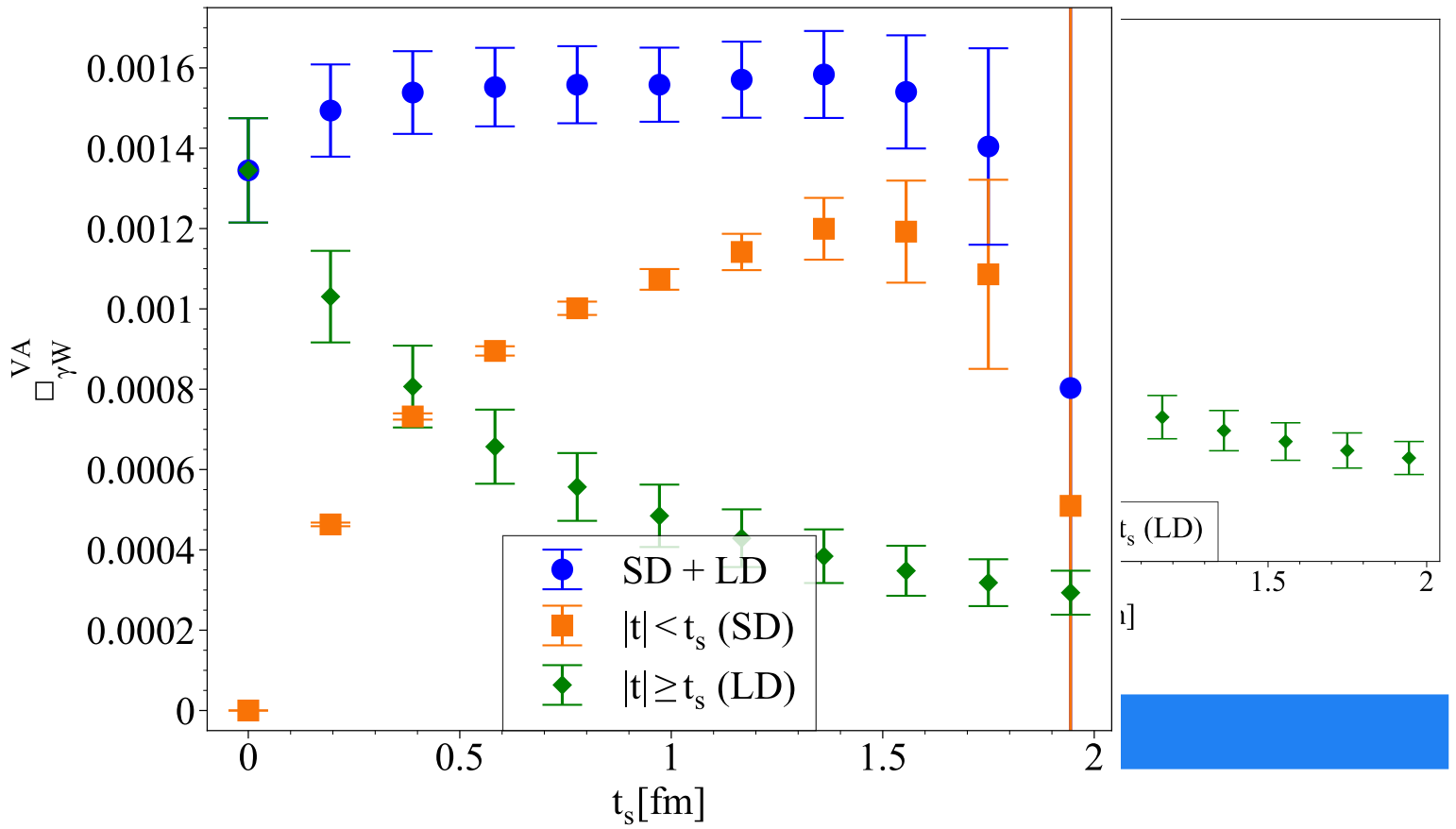

Long Distance (LD)

Plateau after IVR

Substitution Method

$$\Box_{\gamma W}^{VA} = \frac{3\alpha_e}{2\pi} \int \frac{dQ^2}{Q^2} \frac{m_W^2}{m_W^2 + Q^2} M_n\left(Q^2\right).$$

- Box term encounters a notably increased noise originating from $M_n(Q^2)$ at small Q^2 region.
- we can use the model-independent relation:

$$\int d^3\vec{x}\bar{H}\left(t_g, \vec{x}\right) = -3\,\mathring{g}_A\left(\mathring{\mu}_p + \mathring{\mu}_n\right)$$

	24D	32Dfine	Cont.	PDG
$-3g_A(\mu_p + \mu_n)$	-3.31(49)	-3.02(53)	-2.65(1.31)	-3.366(3)

Substitution Method

$$\Box_{\gamma W}^{VA} = \frac{3\alpha_e}{2\pi} \int \frac{dQ^2}{Q^2} \frac{m_W^2}{m_W^2 + Q^2} M_n\left(Q^2\right).$$

- Box term encounters a notably increased noise originating from $M_n(Q^2)$ at small Q^2 region.
- we can use the model-independent relation:

$$\int d^3\vec{x}\bar{H}\left(t_g, \vec{x}\right) = -3\,\mathring{g}_A\left(\mathring{\mu}_p + \mathring{\mu}_n\right)$$

	24D	32Dfine	Cont.	PDG
$-3g_A(\mu_p+\mu_n)$	-3.31(49)	-3.02(53)	-2.65(1.31)	-3.366(3)

$$M_n^{\mathrm{LD}} = -\frac{1}{6}\frac{\sqrt{Q^2}}{m_N}\int d^3\vec{x}\,\left[\tilde{\omega}(t_s,\vec{x}) - \tilde{\omega}_0\right]\bar{H}(t_g,\vec{x}) + \frac{1}{2}\frac{\sqrt{Q^2}}{m_N}\tilde{\omega}_0 g_A(\mu_p+\mu_n).$$

Substitution Method

$$\Box_{\gamma W}^{VA} = \frac{3\alpha_e}{2\pi} \int \frac{dQ^2}{Q^2} \frac{m_W^2}{m_W^2 + Q^2} M_n\left(Q^2\right).$$

北京大学 PEKING UNIVERSITY

- Box term encounters a notably increased noise originating from $M_n(Q^2)$ at small Q^2 region.
- we can use the model-independent relation:

$$\int d^3\vec{x}\bar{H}\left(t_g, \vec{x}\right) = -3\,\mathring{g}_A\left(\mathring{\mu}_p + \mathring{\mu}_n\right)$$

	24D	32Dfine	Cont.	PDG
$-3g_A(\mu_p+\mu_n)$	-3.31(49)	-3.02(53)	-2.65(1.31)	-3.366(3)

$$M_n^{\mathrm{LD}} = -\frac{1}{6}\frac{\sqrt{Q^2}}{m_N}\int d^3\vec{x}\,\left[\tilde{\omega}(t_s,\vec{x}) - \tilde{\omega}_0\right]\bar{H}(t_g,\vec{x}) + \frac{1}{2}\frac{\sqrt{Q^2}}{m_N}\tilde{\omega}_0 g_A(\mu_p+\mu_n).$$

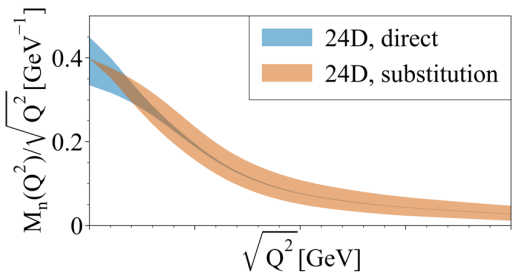

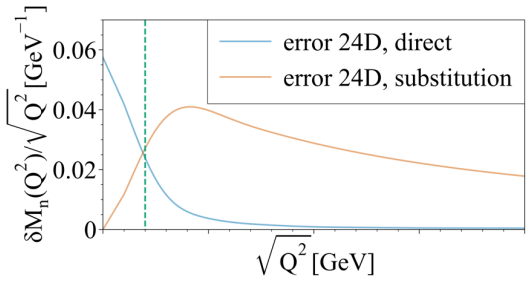

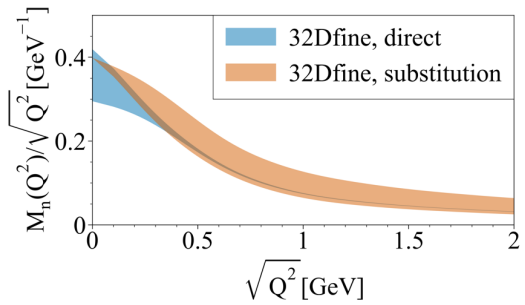

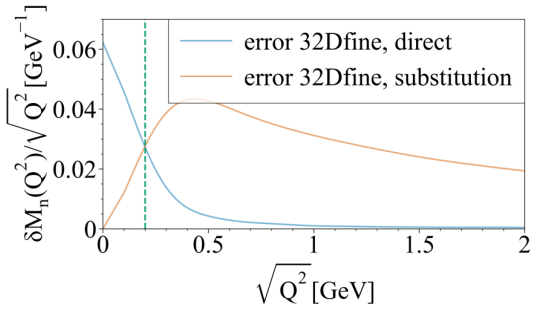

Substitution Method

$$\Box_{\gamma W}^{VA} = \frac{3\alpha_e}{2\pi} \int \frac{dQ^2}{Q^2} \frac{m_W^2}{m_W^2 + Q^2} M_n\left(Q^2\right).$$

北京大学 PEKING UNIVERSITY

- Box term encounters a notably increased noise originating from $M_n(Q^2)$ at small Q^2 region.

- we can use the model-independent relation:

$$\int d^3\vec{x}\bar{H}\left(t_g, \vec{x}\right) = -3\,\mathring{g}_A\left(\mathring{\mu}_p + \mathring{\mu}_n\right)$$

	24D	32Dfine	Cont.	PDG
$-3g_A(\mu_p+\mu_n)$	-3.31(49)	-3.02(53)	-2.65(1.31)	-3.366(3)

$$M_n^{\mathrm{LD}} = -\frac{1}{6}\frac{\sqrt{Q^2}}{m_N}\int d^3\vec{x}\,\left[\tilde{\omega}(t_s,\vec{x}) - \tilde{\omega}_0\right]\bar{H}(t_g,\vec{x}) + \frac{1}{2}\frac{\sqrt{Q^2}}{m_N}\tilde{\omega}_0 g_A(\mu_p+\mu_n).$$

- There exists a uniform scale $Q_0 = 0.2$ GeV, when $Q<Q_0$ the substitution method exhibits superiority.

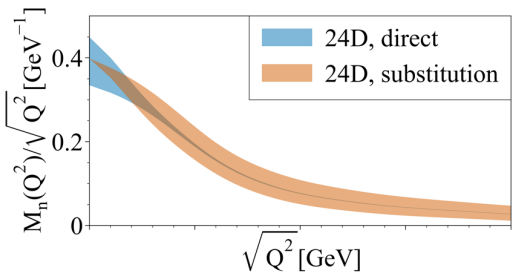

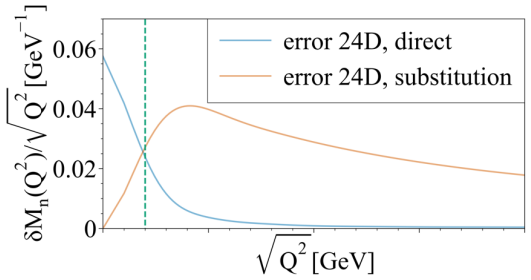

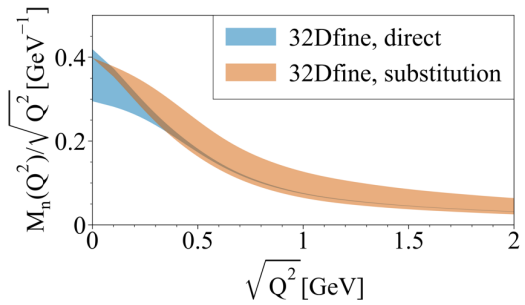

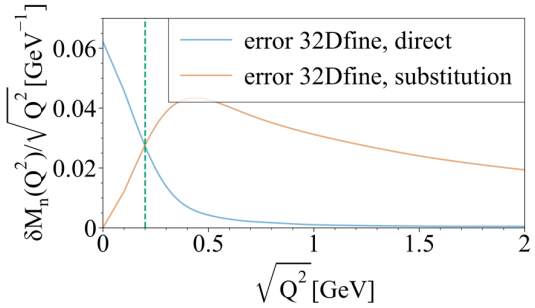

Numerical Result

北京大学 PEKING UNIVERSITY

➢ We use two lattice ensembles generated by RBC and UKQCD Collaborations and both of them have physical pion mass:

ensemble	M_π/MeV	$L^3 \times T$	a/fm	L·a/fm	N_{conf}
24D	141.2(4)	$24^3 \times 64$	0.1944	4.665	207
32D-fine	143.0(3)	$32^3 \times 64$	0.1432	4.582	69

Numerical Result

北京大学 PEKING UNIVERSITY

➢ We use two lattice ensembles generated by RBC and UKQCD Collaborations and both of them have physical pion mass:

ensemble	M_π/MeV	$L^3 \times T$	a/fm	L·a/fm	N_{conf}
24D	141.2(4)	$24^3 \times 64$	0.1944	4.665	207
32D-fine	143.0(3)	$32^3 \times 64$	0.1432	4.582	69

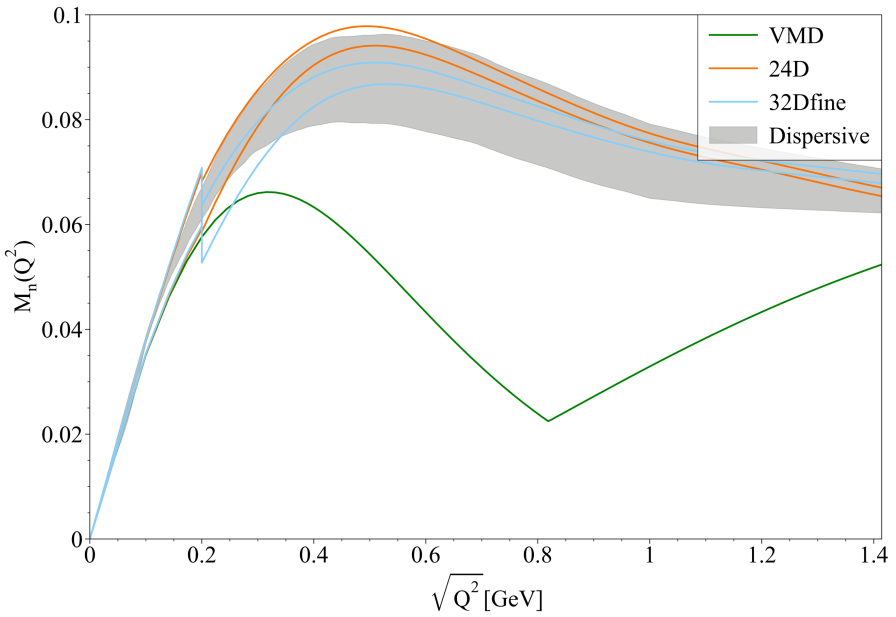

Numerical Result

北京大学 PEKING UNIVERSITY

➢ We use two lattice ensembles generated by RBC and UKQCD Collaborations and both of them have physical pion mass:

ensemble	M_π/MeV	$L^3 \times T$	a/fm	L·a/fm	N_{conf}
24D	141.2(4)	$24^3 \times 64$	0.1944	4.665	207
32D-fine	143.0(3)	$32^3 \times 64$	0.1432	4.582	69

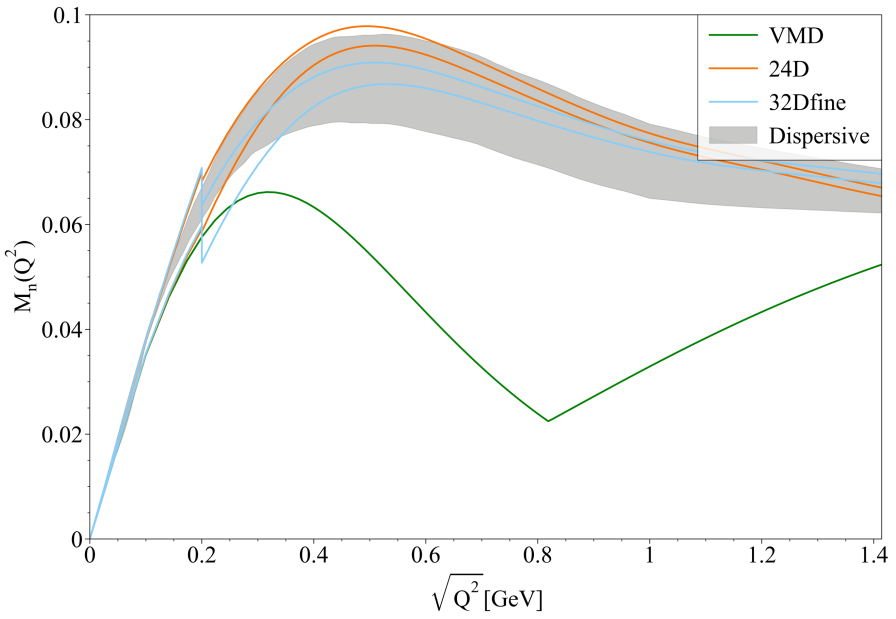

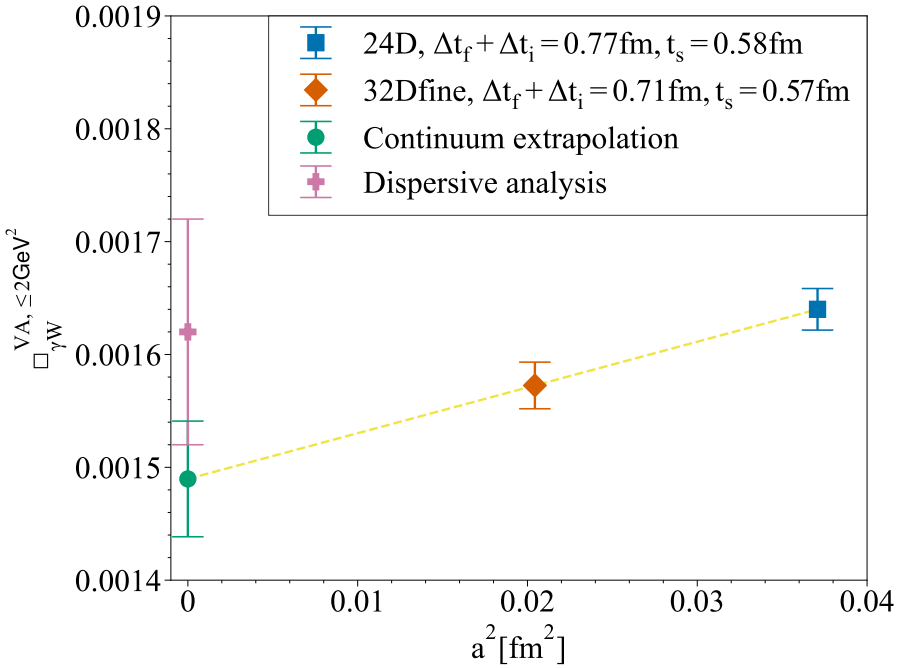

Numerical Result

北京大学 PEKING UNIVERSITY

➢ We use two lattice ensembles generated by RBC and UKQCD Collaborations and both of them have physical pion mass:

ensemble	M_π/MeV	$L^3 \times T$	a/fm	L·a/fm	N_{conf}
24D	141.2(4)	$24^3 \times 64$	0.1944	4.665	207
32D-fine	143.0(3)	$32^3 \times 64$	0.1432	4.582	69

$$\Delta_R^V = 0.02439(15)_{\text{lat}}(10)_{\text{HO}},$$
$$|V_{ud}| = 0.97386(11)_{\text{exp}}(9)_{\text{RC}}(27)_{\text{NS}}$$
$$|V_{ud}|^2 + |V_{us}|^2 + |V_{ub}|^2 = 0.9987(6)_{V_{ud}}(4)_{V_{us}}.$$

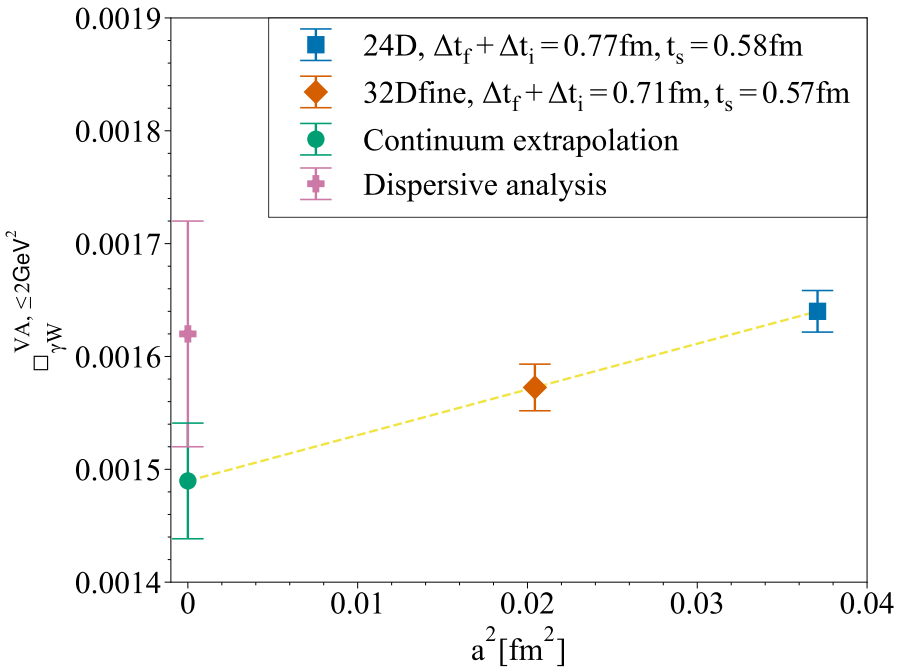

Summary

北京大学 PEKING UNIVERSITY

- The first lattice calculation of γW-box correction was successfully conducted in the pion channel and has been confirmed by an independent lattice calculation.
- We perform the first realistic lattice QCD calculation of the universal γW-box correction to both super-allowed nuclear and neutron beta decays.
- We incorporate long-distance contributions to the hadronic function using the infinite-volume reconstruction(IVR) method.
- Our calculation tends to decrease CKM discrepancy (~ 1.8 σ).
- Better error estimation requires configurations with more lattice spacings of different sizes as input.